Supporting Information for

Electrocatalytic Hydrogen Production by CN- substituted Cobalt Triaryl Corroles

Zheng-Yan Liu[a], Jia-Wei Lai[a], Gang Yang[a], Bao-Ping Ren[a], Zhou-Yan Lv[a], Li-Ping Si[b]*, Hao Zhang[a], Hai-Yang Liu[a]*

**Corresponding author.*

[a] *School of Chemistry and Chemical Engineering, Guangdong Provincial Key Laboratory of Fuel Cell Technology, South China University of Technology, Guangzhou 510641, China.*

E-mail: chhyliu@scut.edu.cn

[b] *School of Materials Science and Energy Engineering, Foshan University, Foshan 528000, China.*

E-mail: lipingsi@fosu.edu.cn (Li-Ping Si).

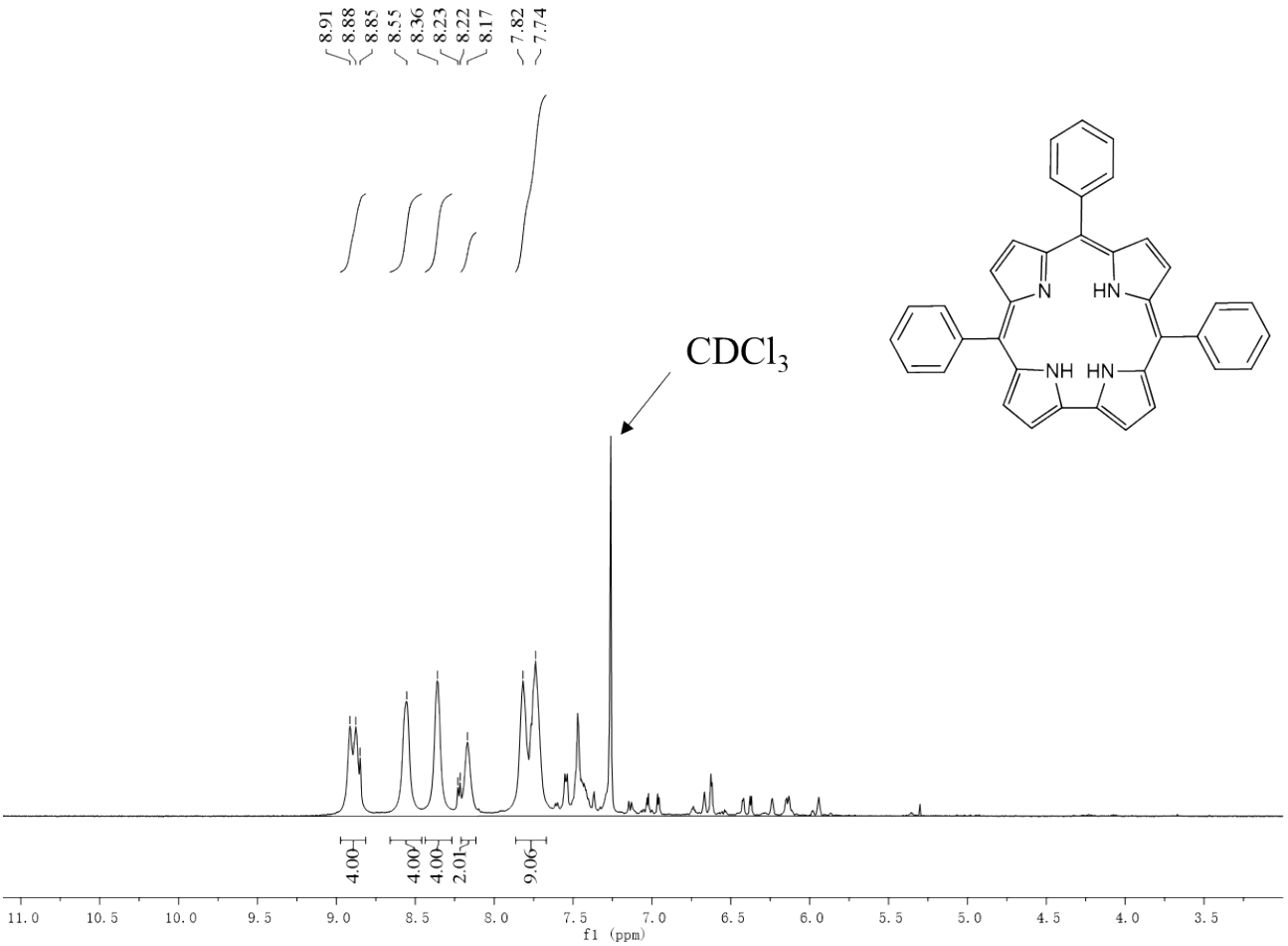

Figure S1 ^{1}H NMR spectrum of TPC

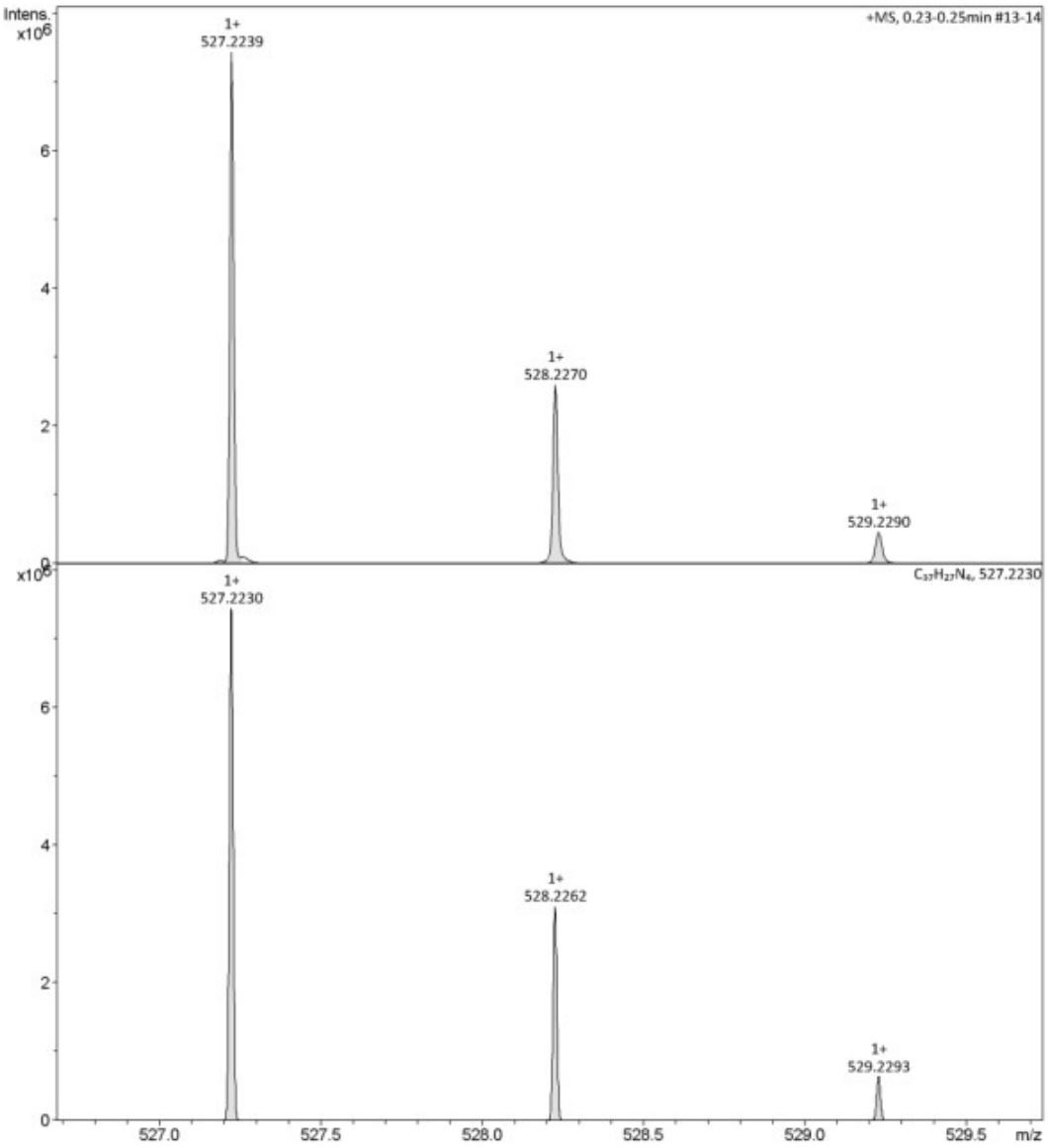

Figure S2 ESI-HRMS spectrum of TPC

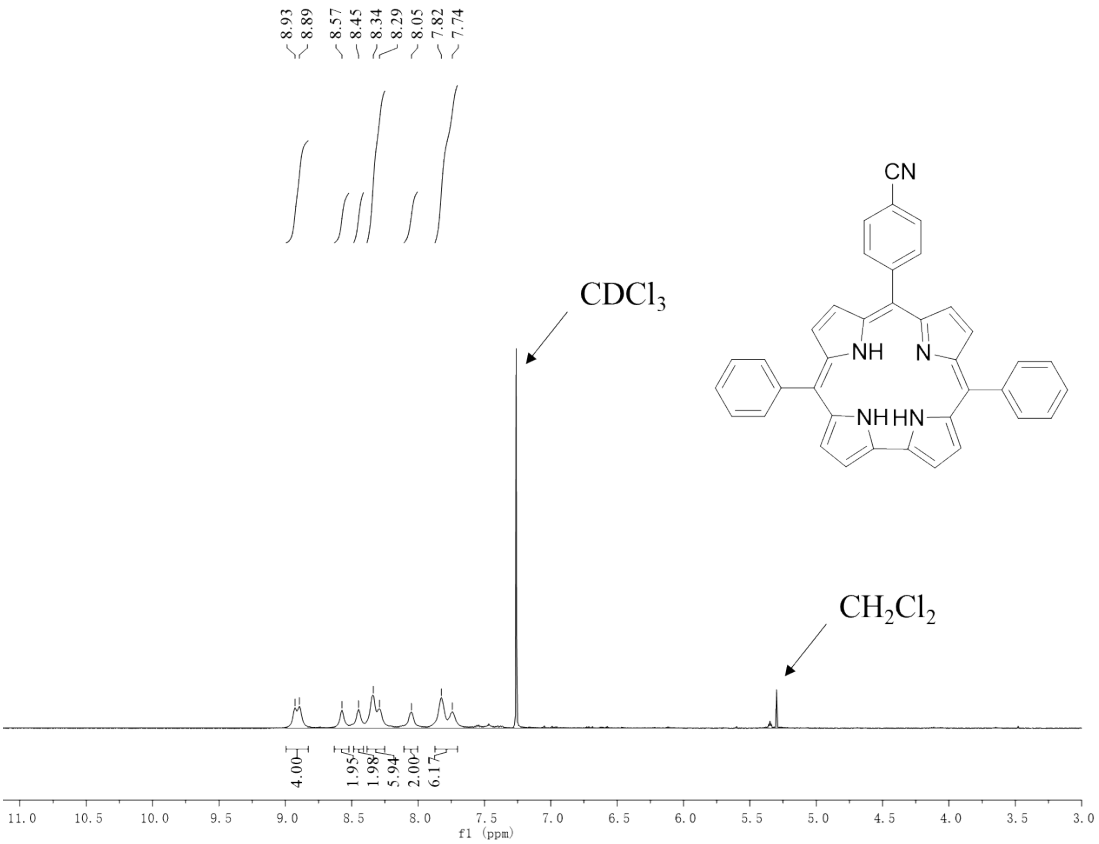

Figure S3 ^{1}H NMR spectrum of BPCC

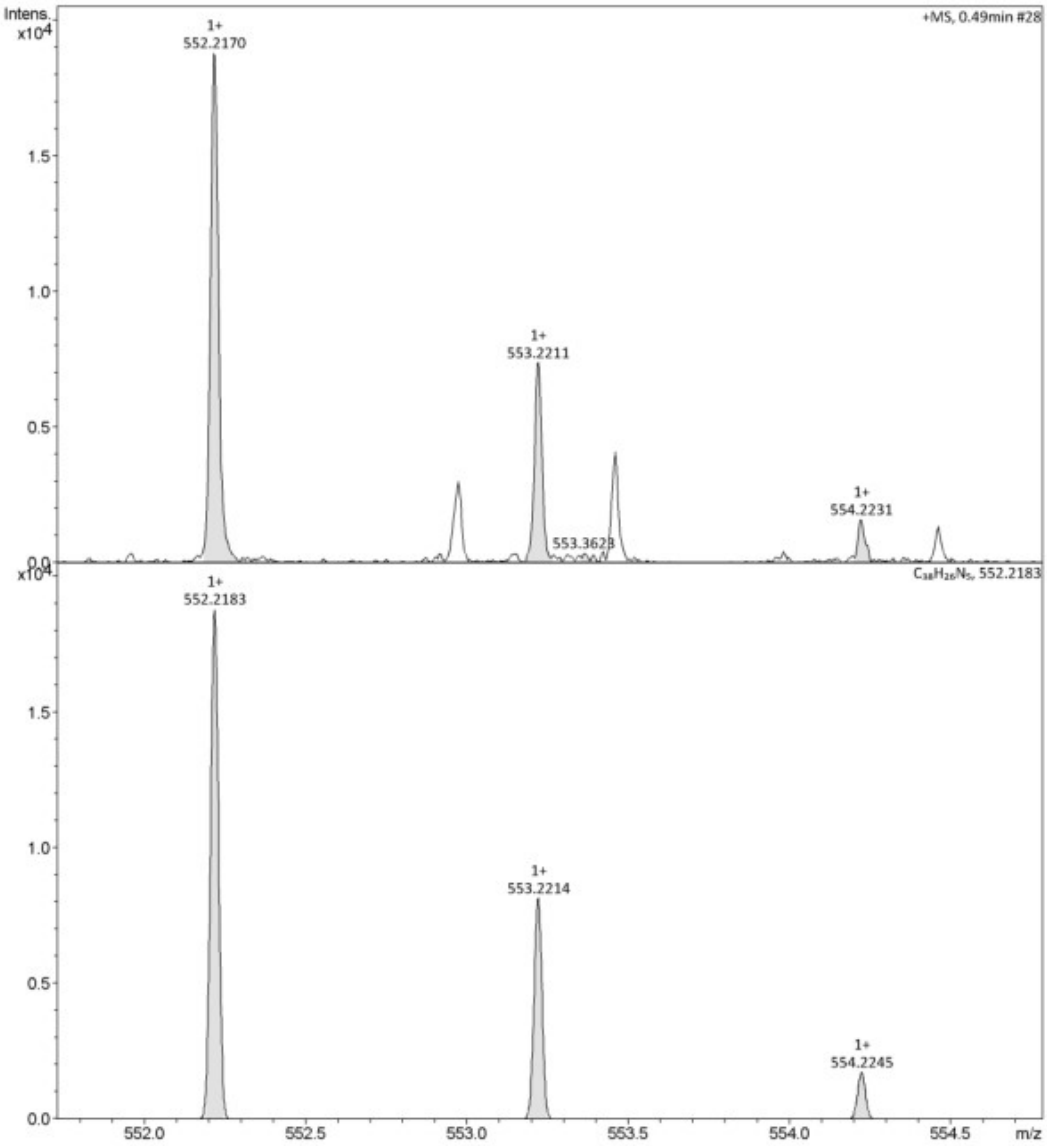

Figure S4 ESI-HRMS spectrum of BPCC

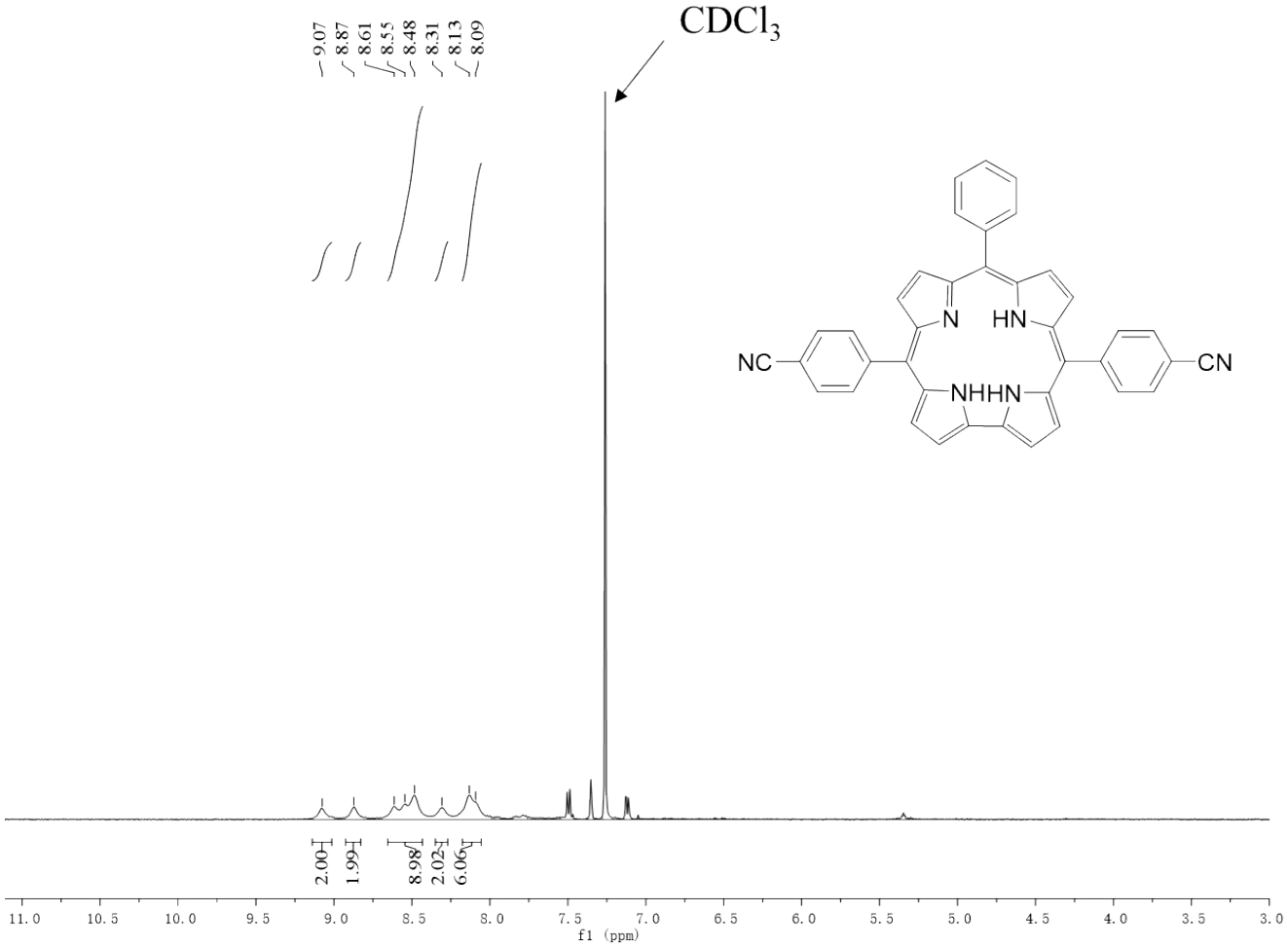

Figure S5 ^{1}H NMR spectrum of PBCC

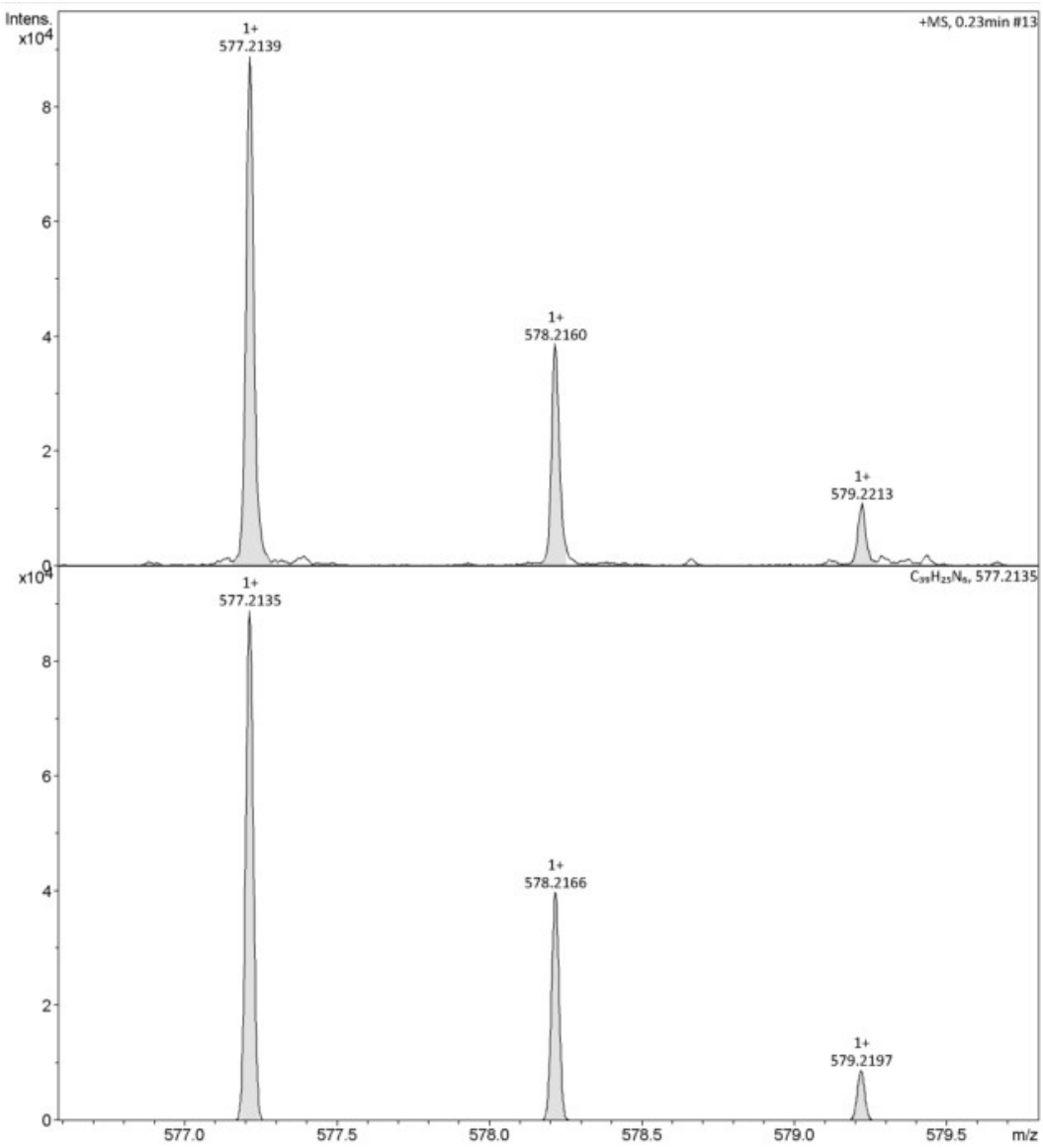

Figure S6 ESI-HRS spectrum of PBCC

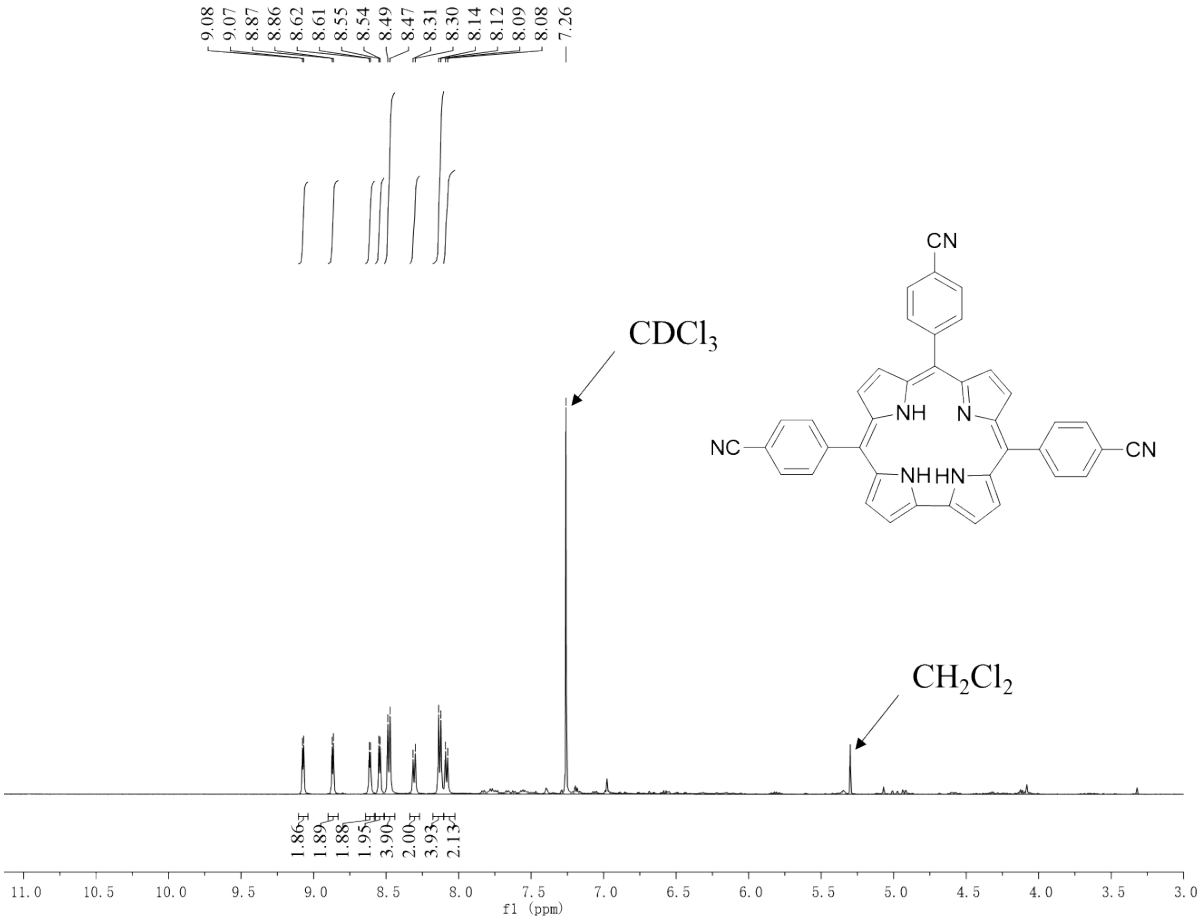

Figure S7 ^{1}H NMR spectrum of TCC

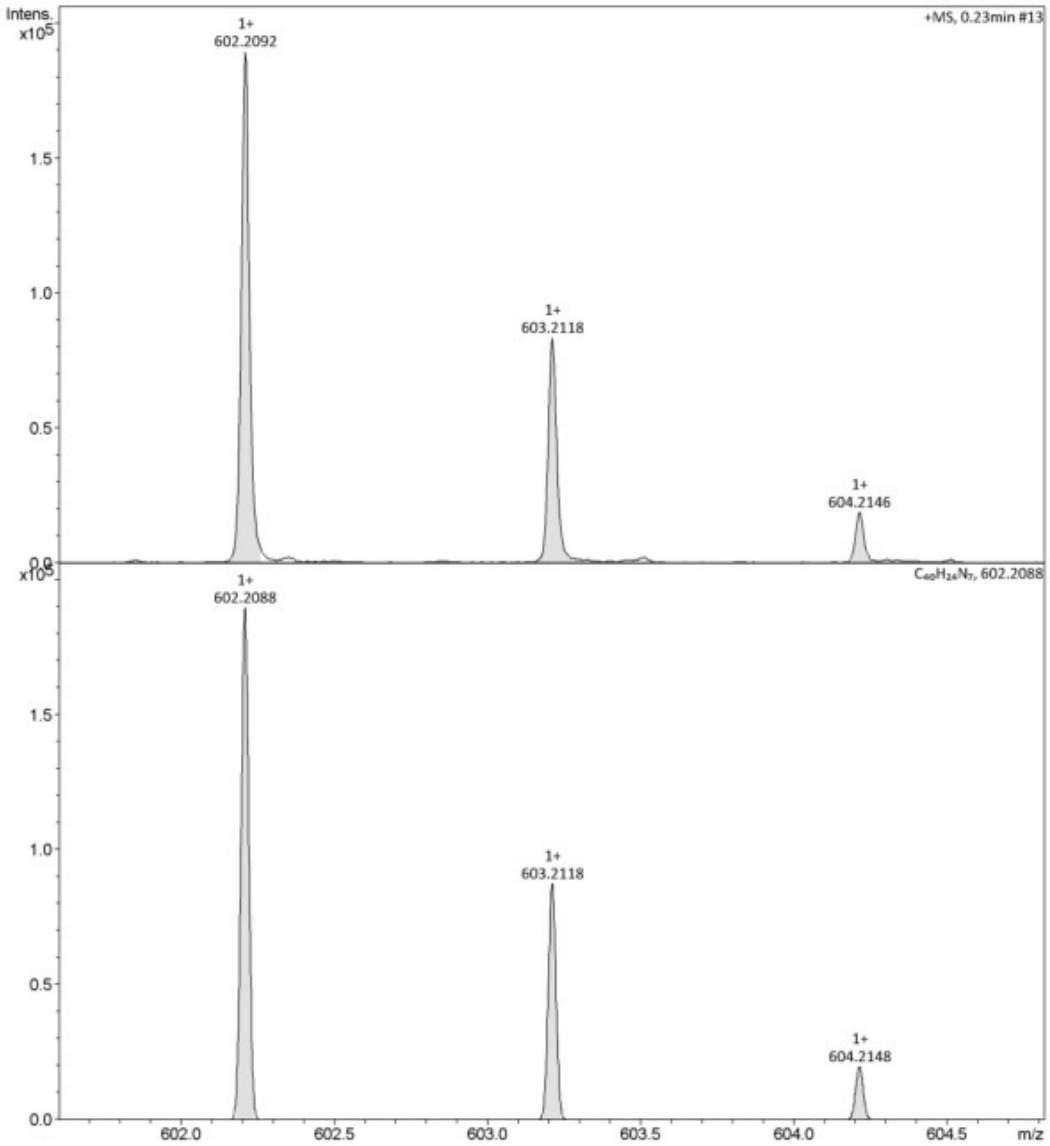

Figure S8 ESI-HRMS spectrum of TCC

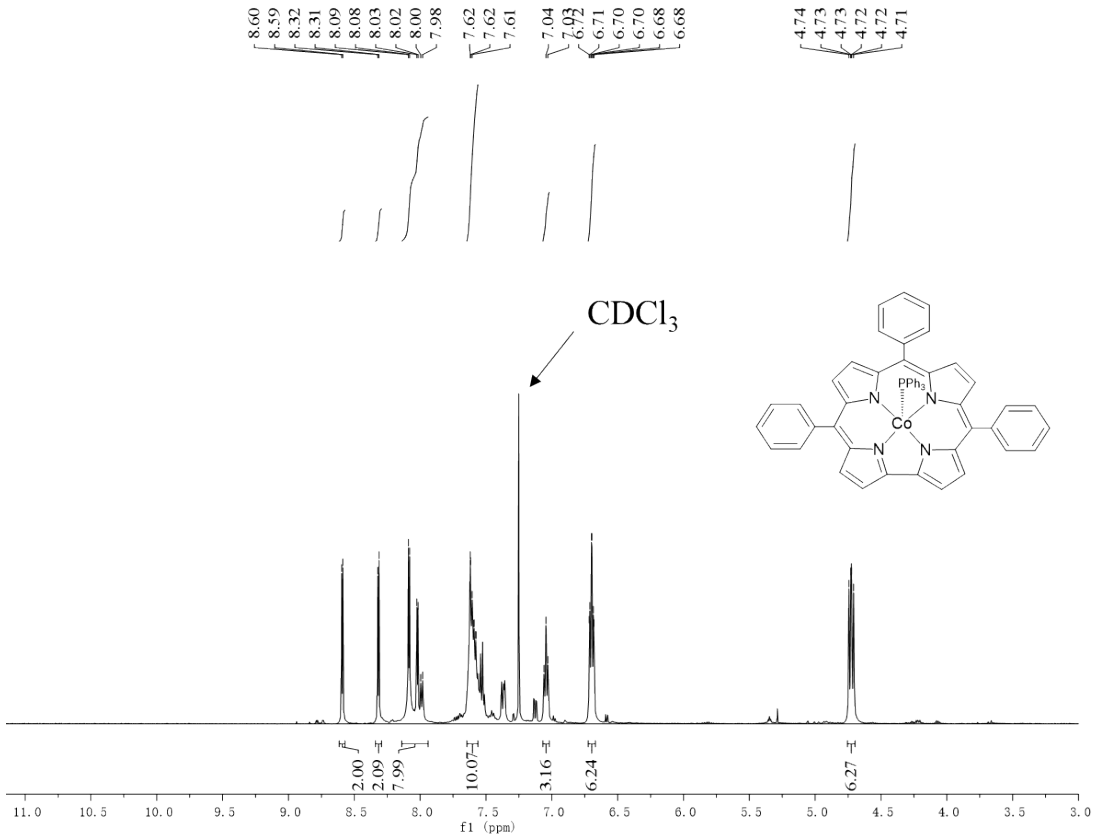

Figure S9 ^{1}H NMR spectrum of complex **1**

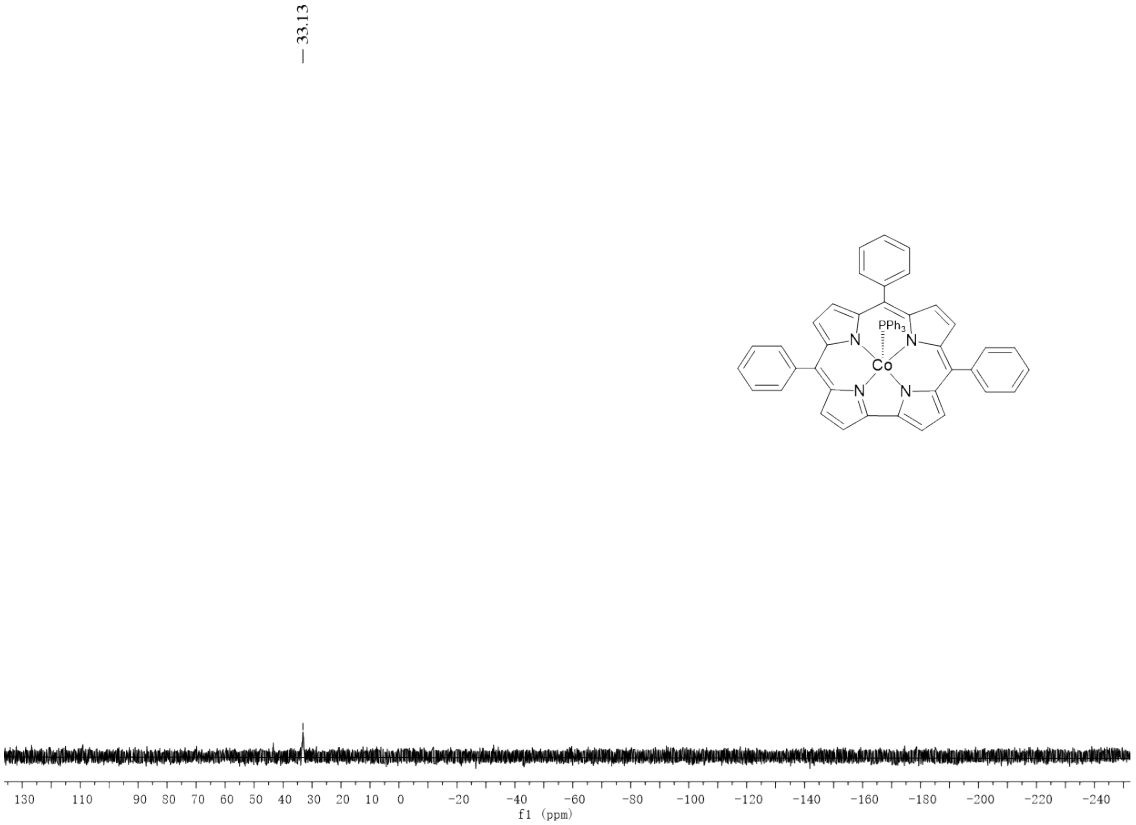

Figure S10 ^{31}P NMR spectrum of complex **1**

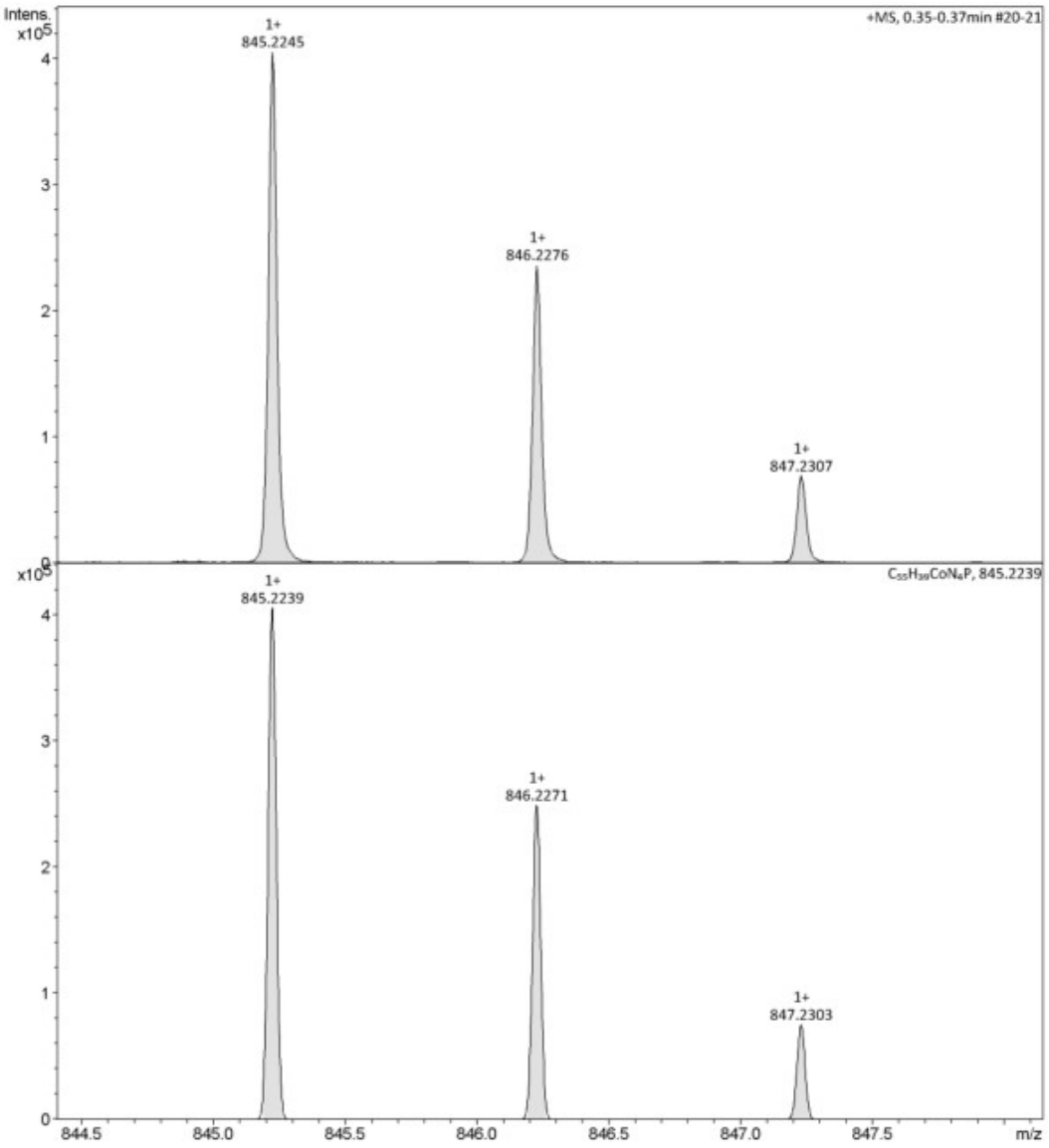

Figure S11 ESI-HRMS spectrum of complex **1**

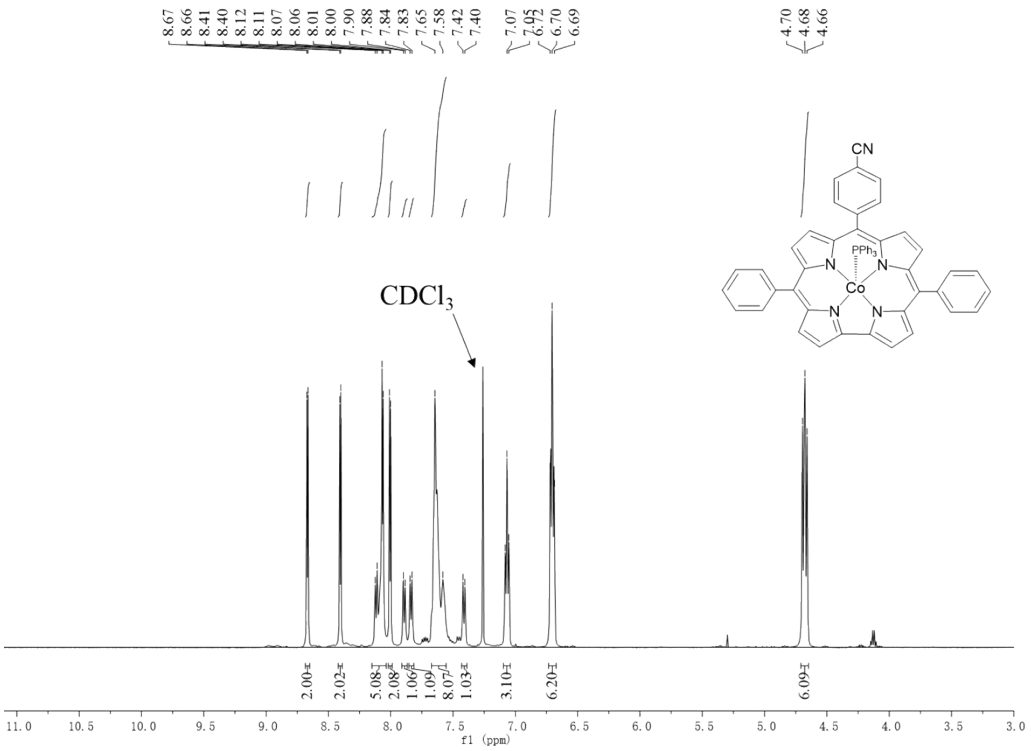

Figure S12 ^{1}H NMR spectrum of complex **2**

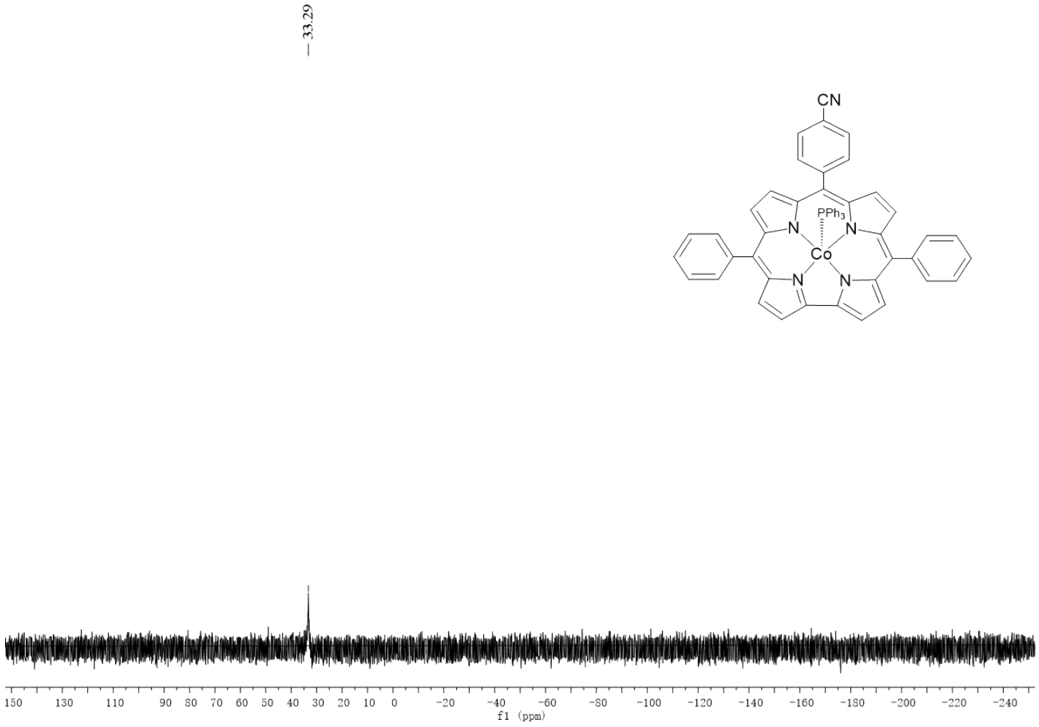

Figure S13 ^{31}P NMR spectrum of complex **2**

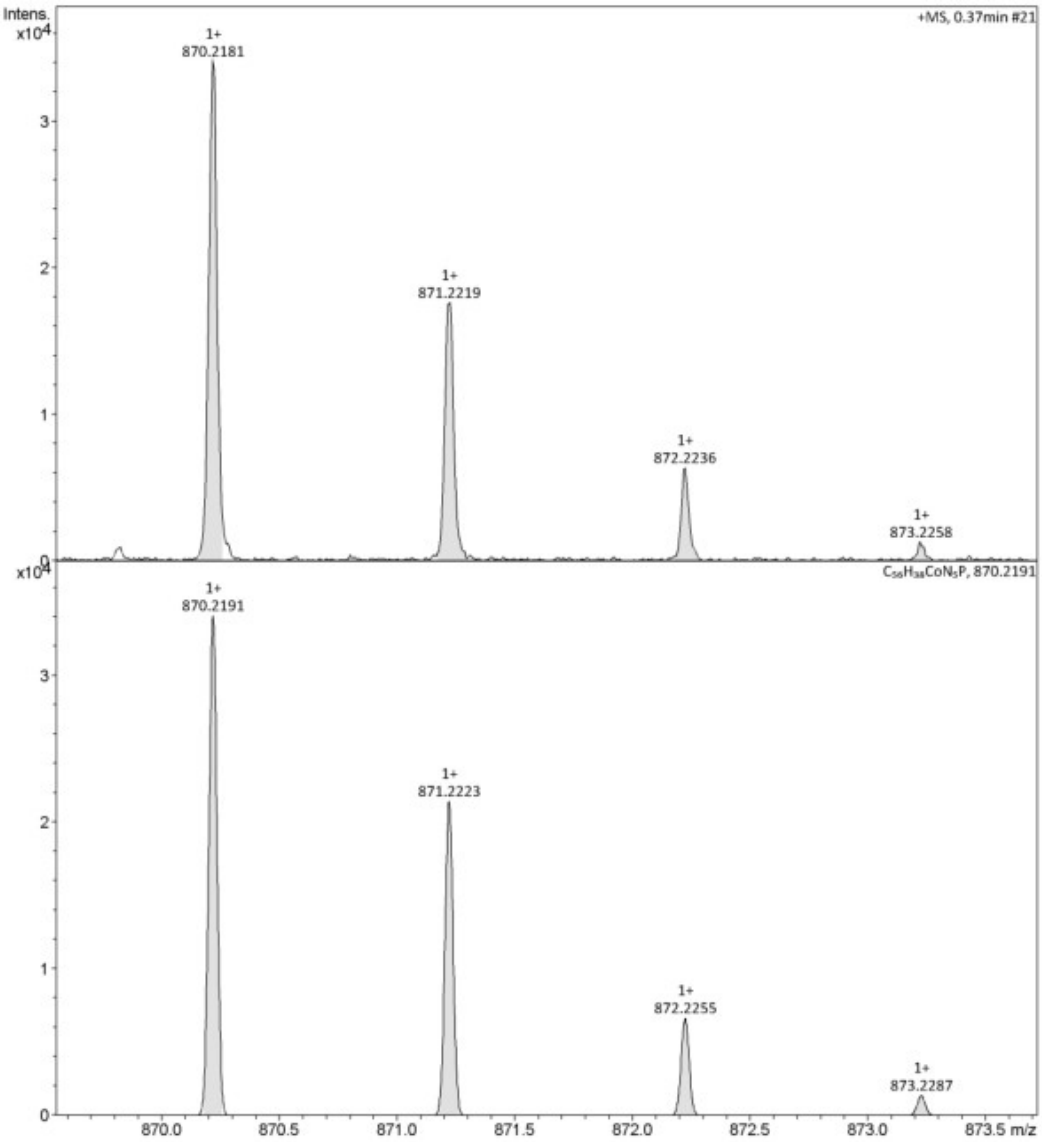

Figure S14 ESI-HRMS spectrum of complex **2**

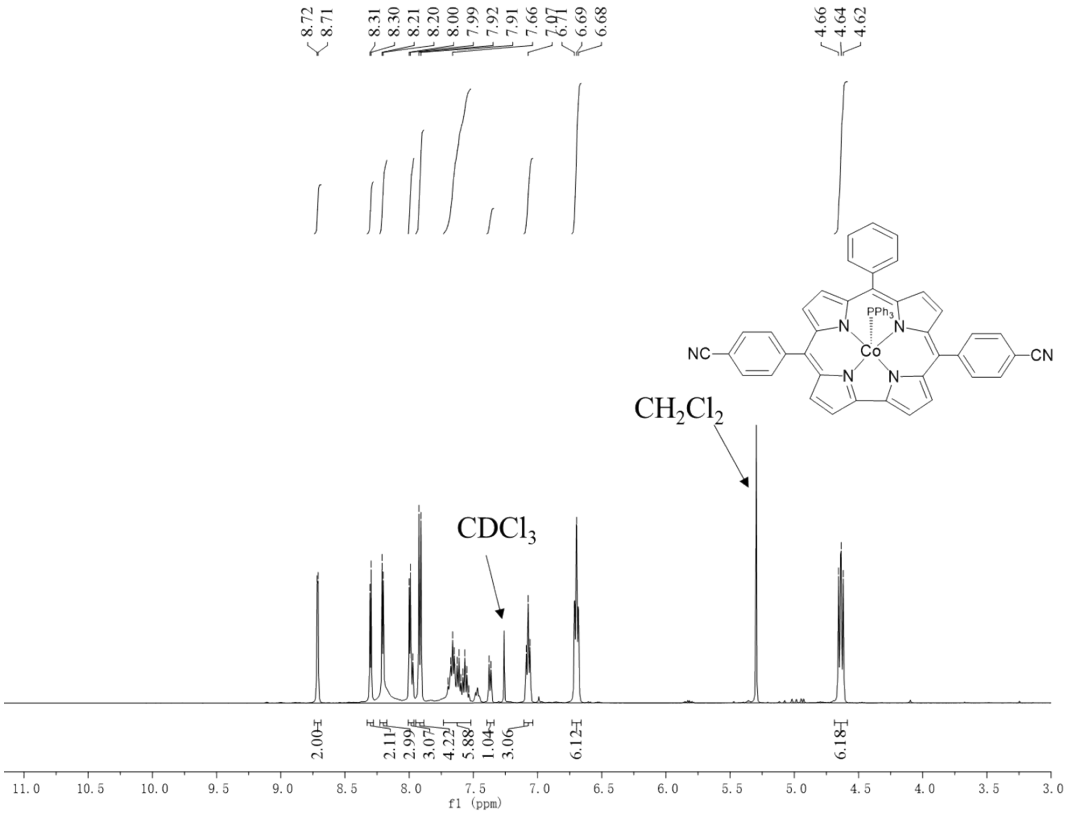

Figure S15 ^{1}H NMR spectrum of complex **3**

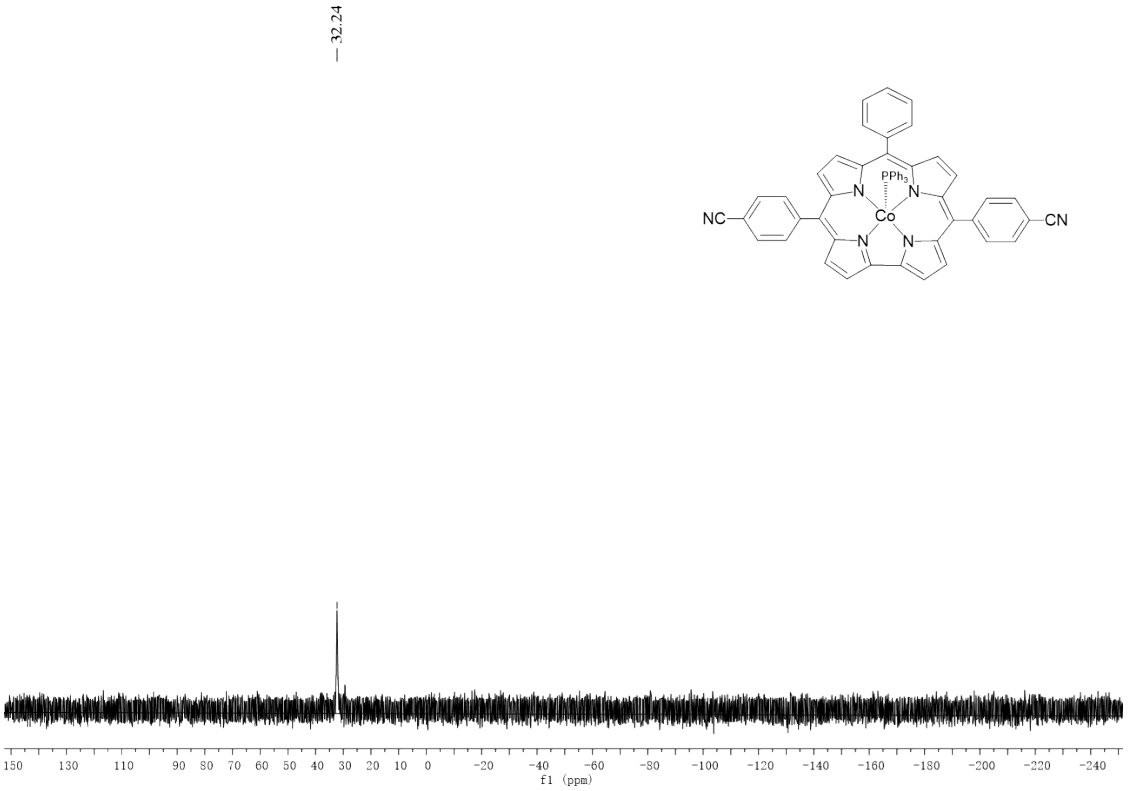

Figure S16 ^{31}P NMR spectrum of complex **3**

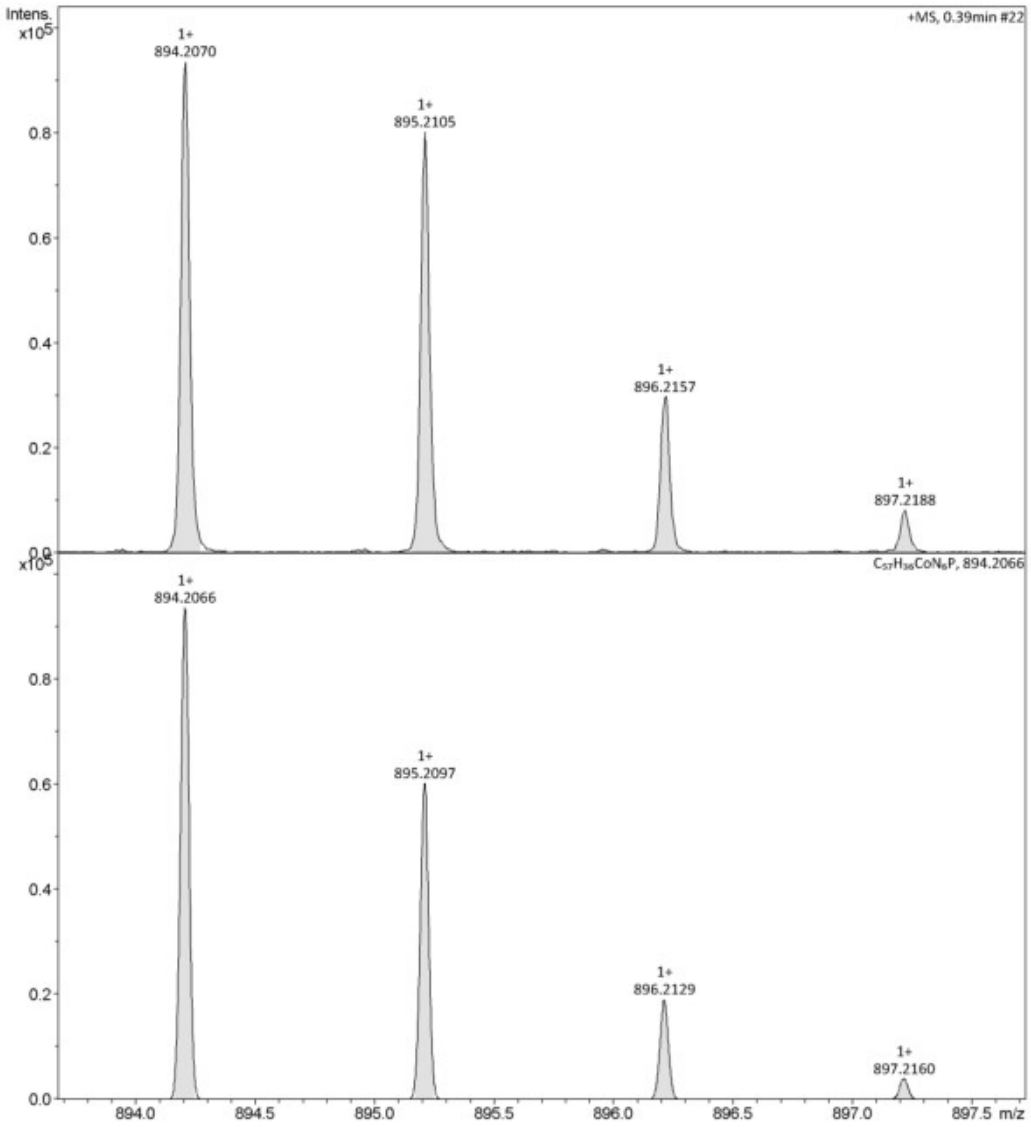

Figure S17 ESI-HRMS spectrum of complex **3**

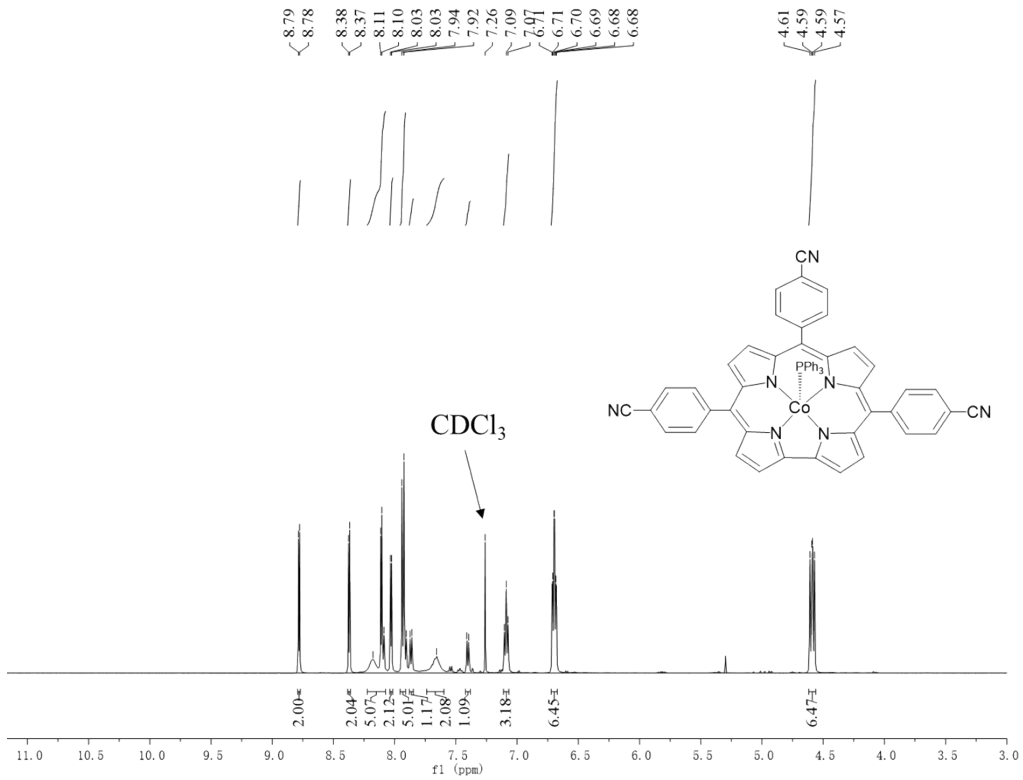

Figure S18 ^{1}H NMR spectrum of complex **4**

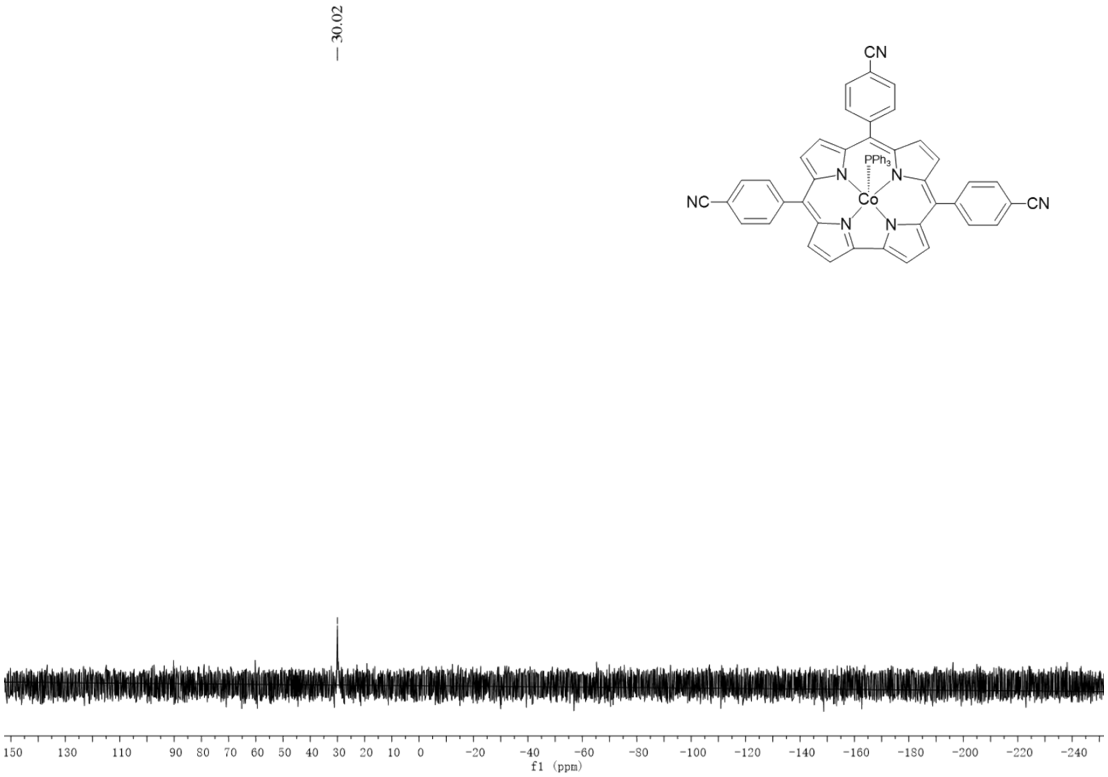

Figure S19 ^{31}P NMR spectrum of complex **4**

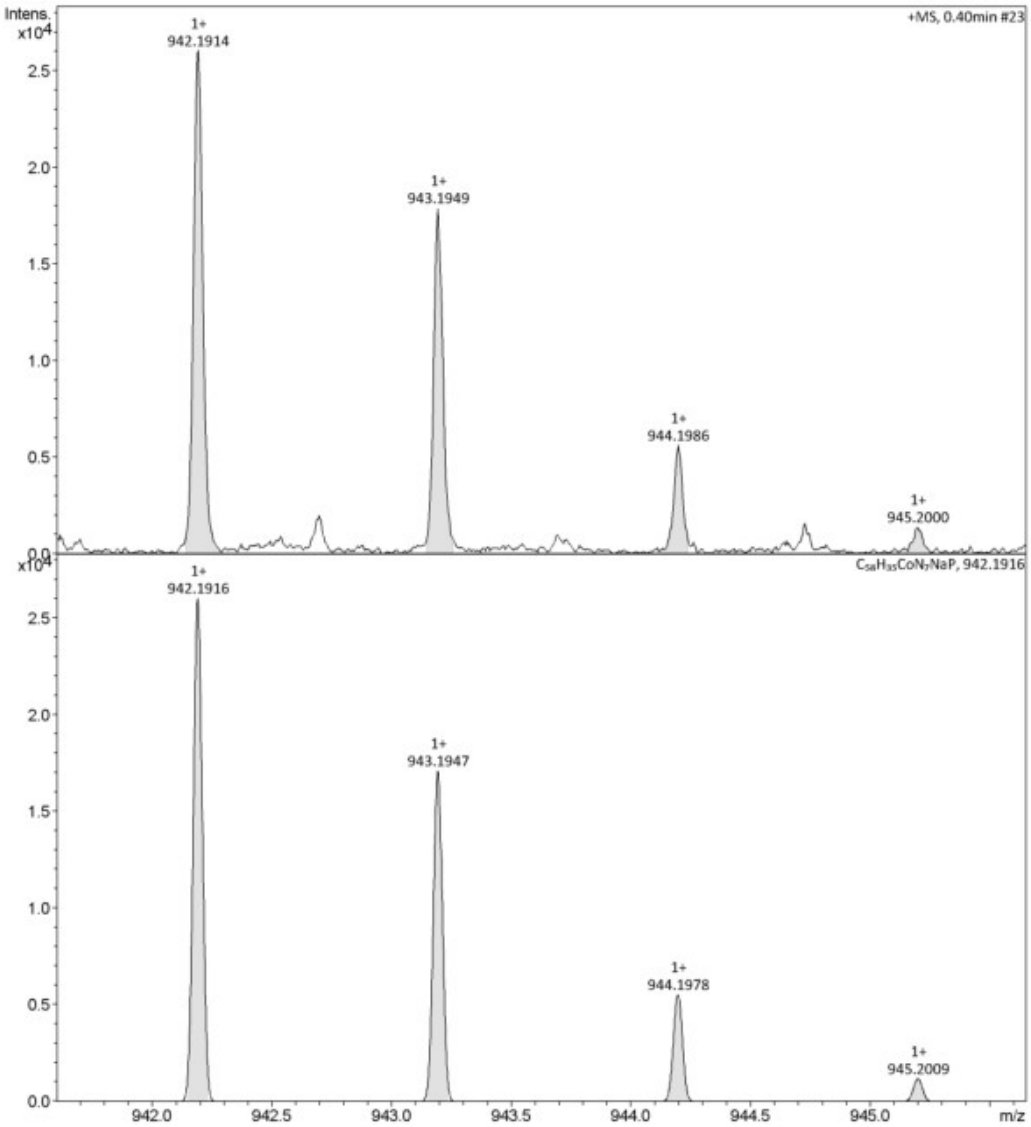

Figure S20 ESI-HRMS spectrum of complex **4**

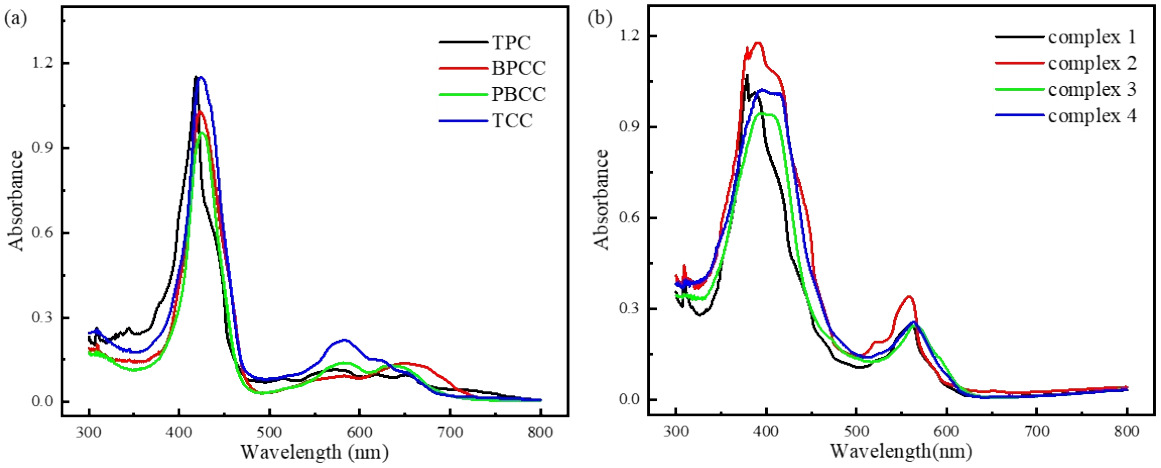

Figure S21 UV-Vis spectrum of free base corroles (TPC, BPCC, PBCC, TCC) and cobalt complexes **1**, **2**, **3, 4** in dichloromethane (DCM).

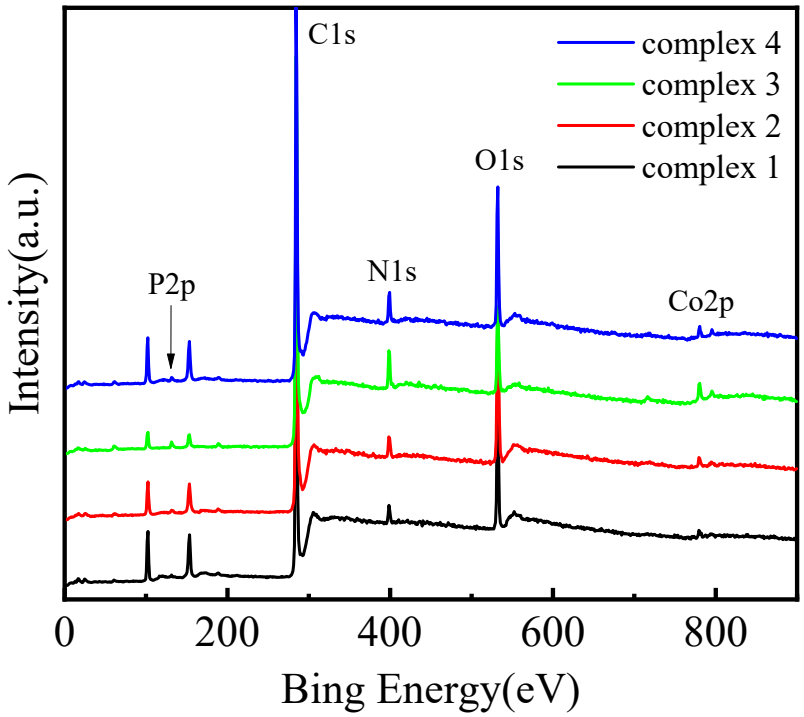

Figure S22 XPS survey spectrum of complex 1,2,3,4

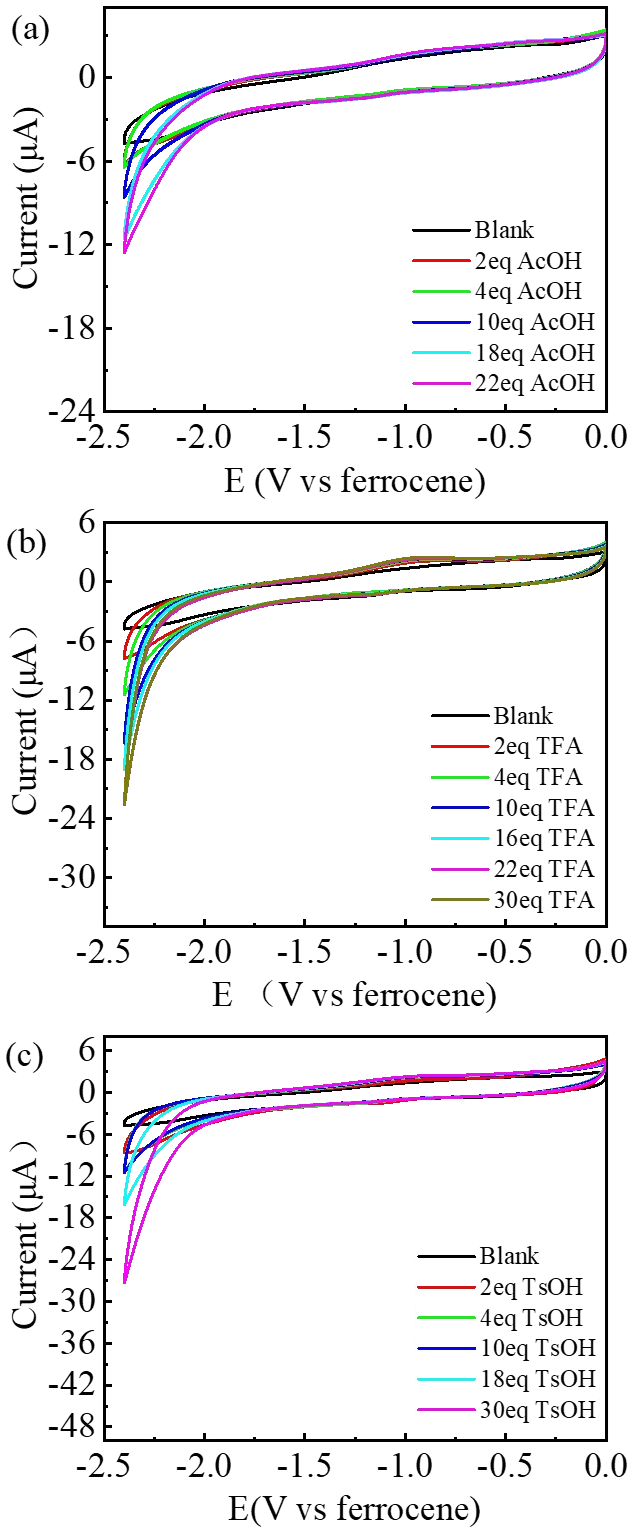

Figure S23 CVs of catalyst-free control experiments with the gradual addition of AcOH(a), TFA(b), TsOH(c) and without cobalt complex.

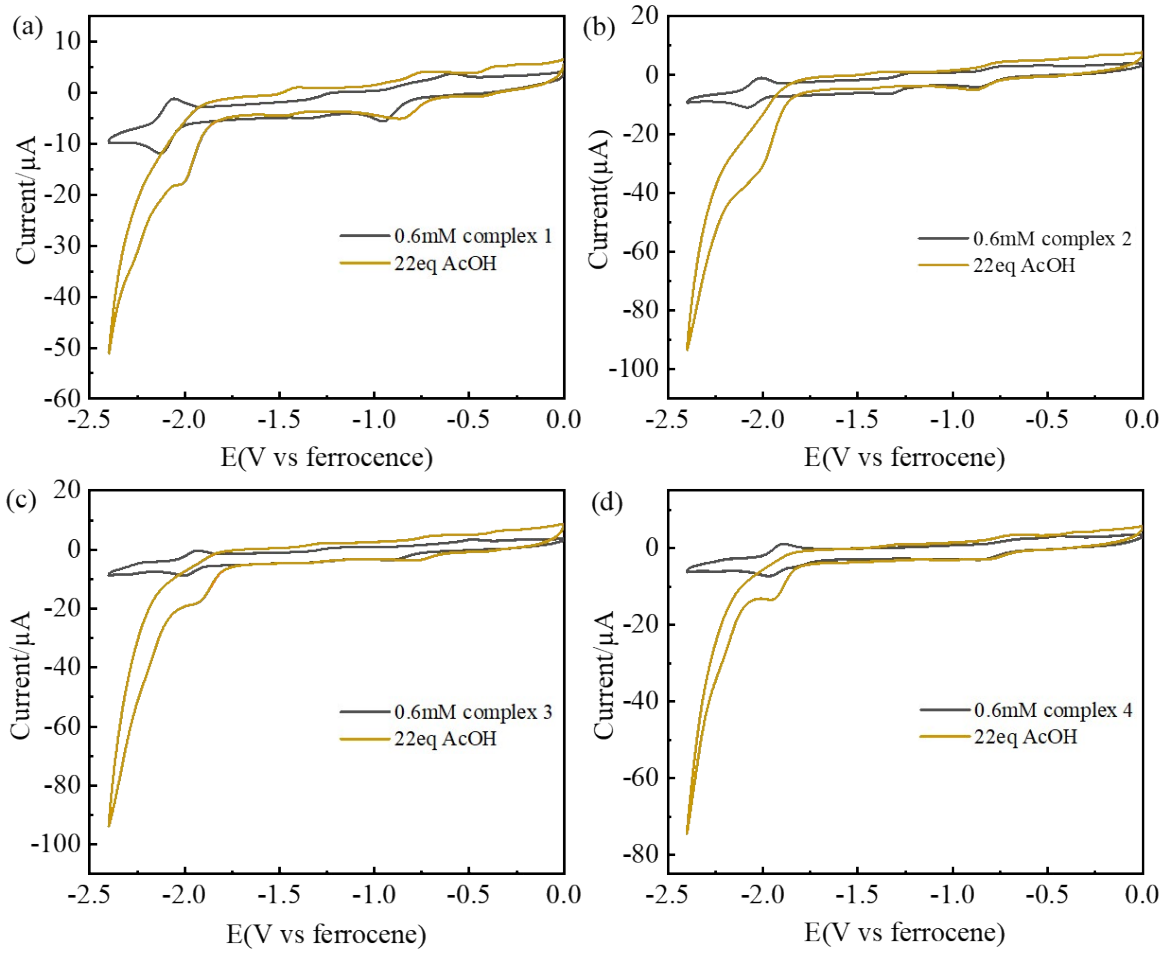

Figure S24 CV of 0.6mM cobalt complex **1**, **2**, **3**, **4** (a, b, c, d) with the addition of 22 equiv AcOH.

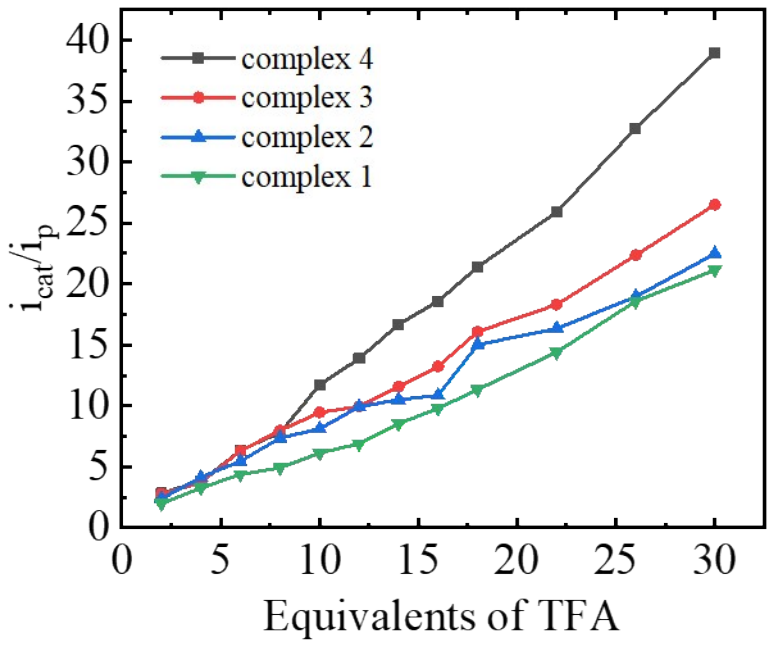

Figure S25 i_{cat}/i_p value of cobalt complex **1**, **2**, **3**, **4** (0.6 mM) in DMF at different trifluoroacetic acid concentrations.

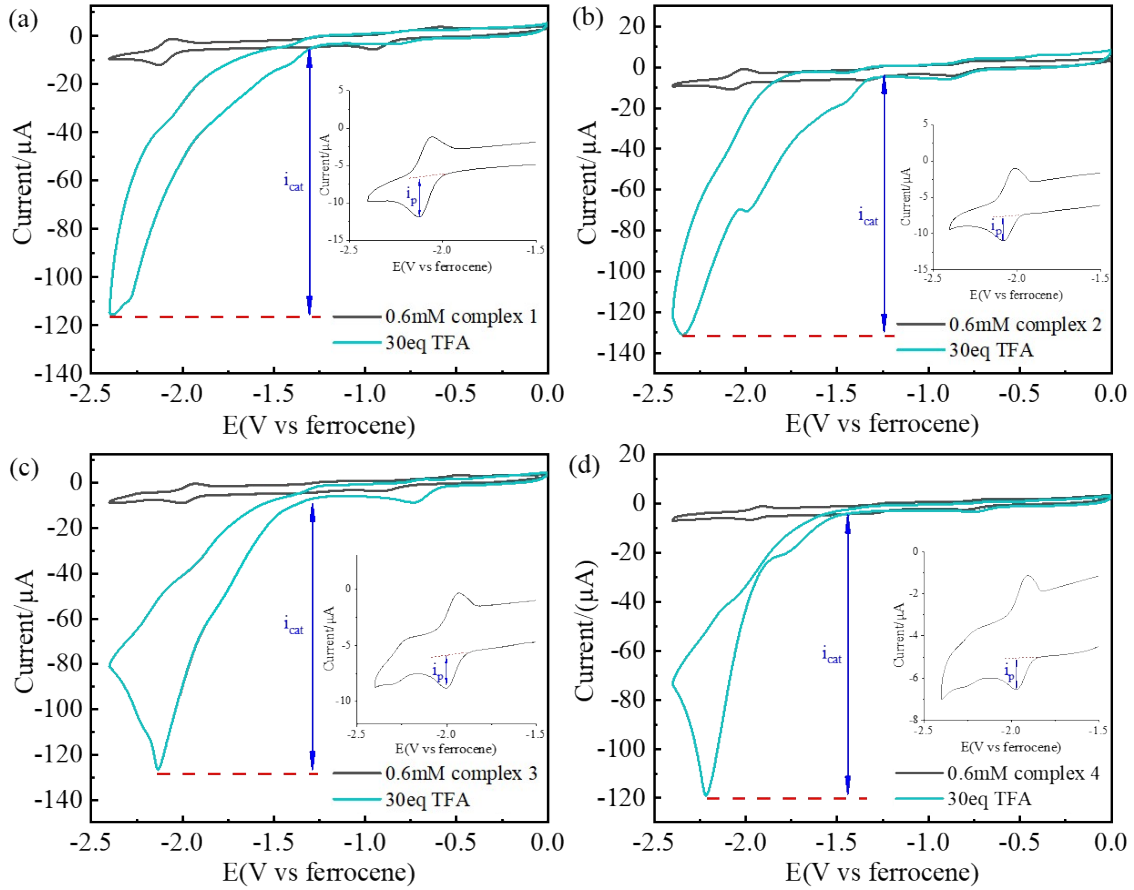

Figure S26 CV of 0.6 mM cobalt complex **1**, **2**, **3**, **4** (a, b, c, d) with the addition of 30 equiv TFA.

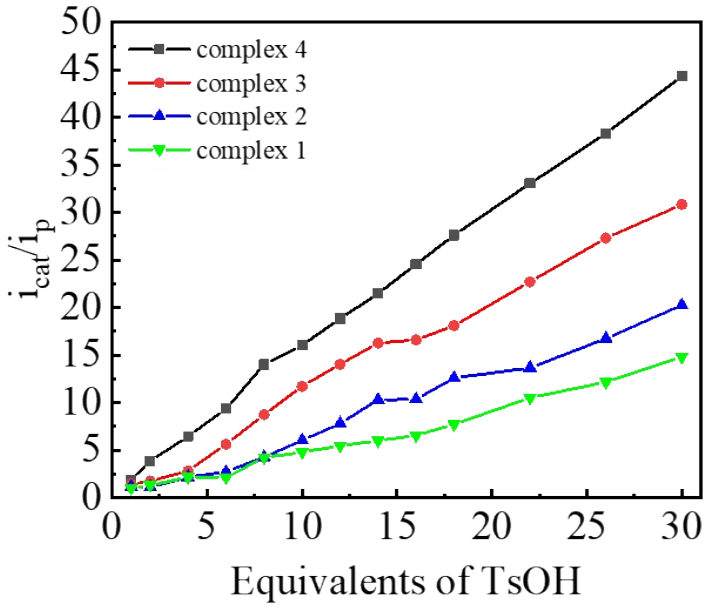

Figure S27 i_{cat}/i_p value of cobalt complex **1**, **2**, **3**, **4** (0.6 mM) in DMF at different p-Toluenesulfonic acid concentrations.

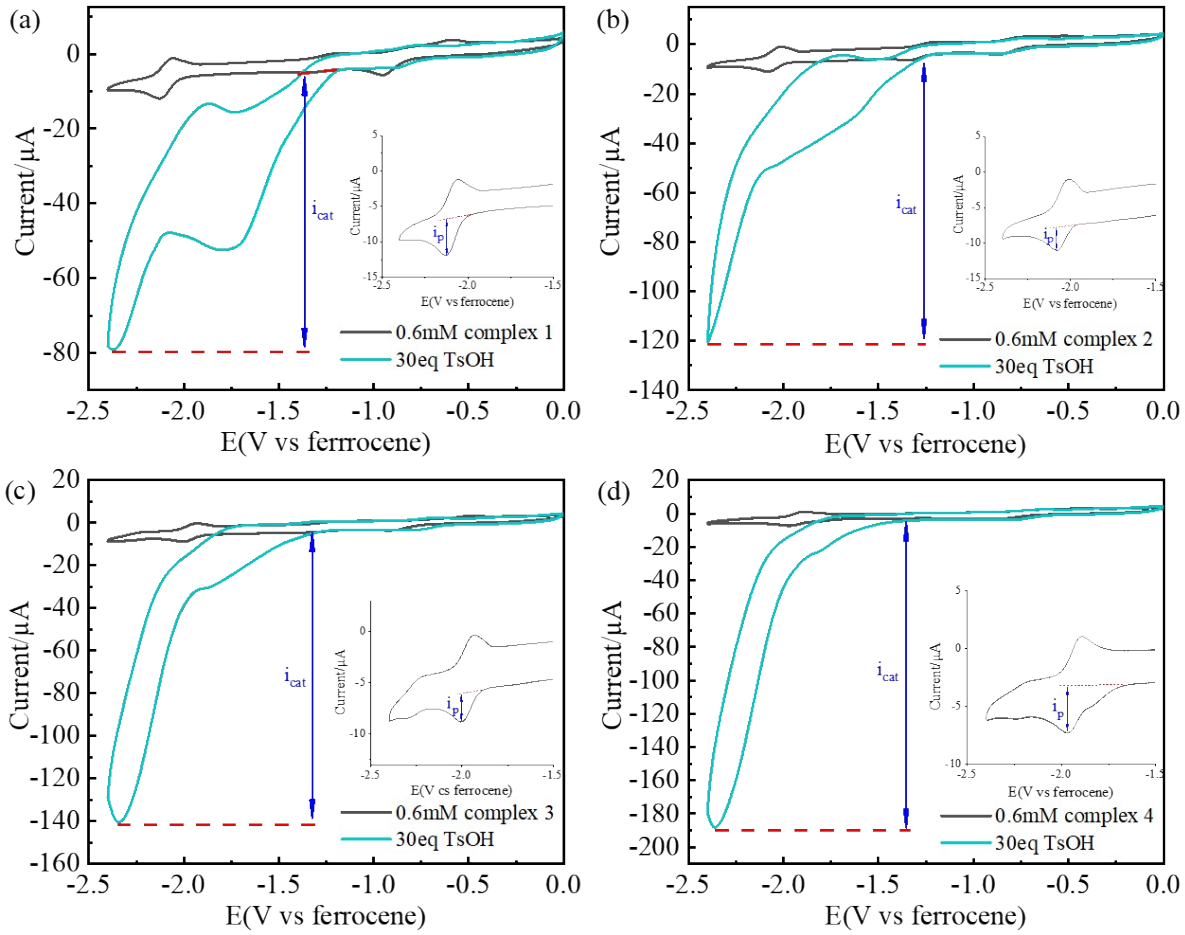

Figure S28 CV of 0.6 mM cobalt complex **1**, **2**, **3**, **4** (a, b, c, d) with the addition of 30 equiv TsOH.

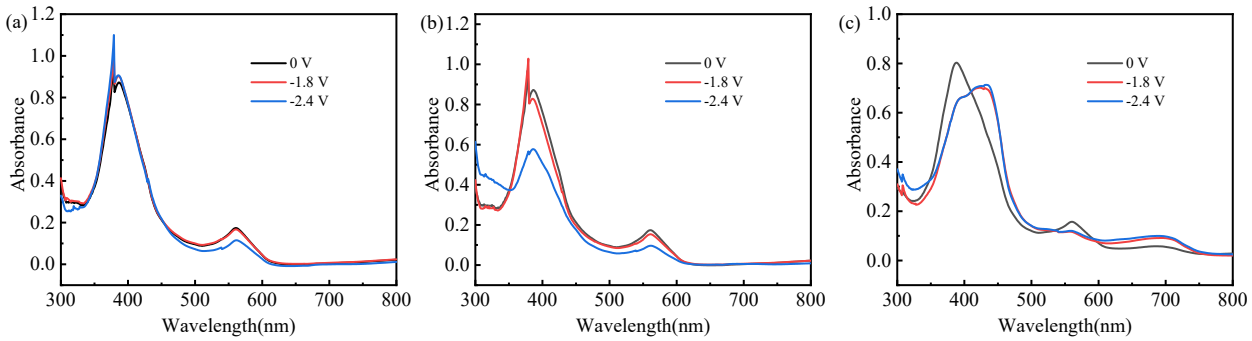

Figure S29 Absorption spectra of complex 1 in DMF with different acid concentration at the fixed potentials after 40 minutes electrolysis. (a) Without acid, (b) Low TsOH concentration, (c) High TsOH concentration.

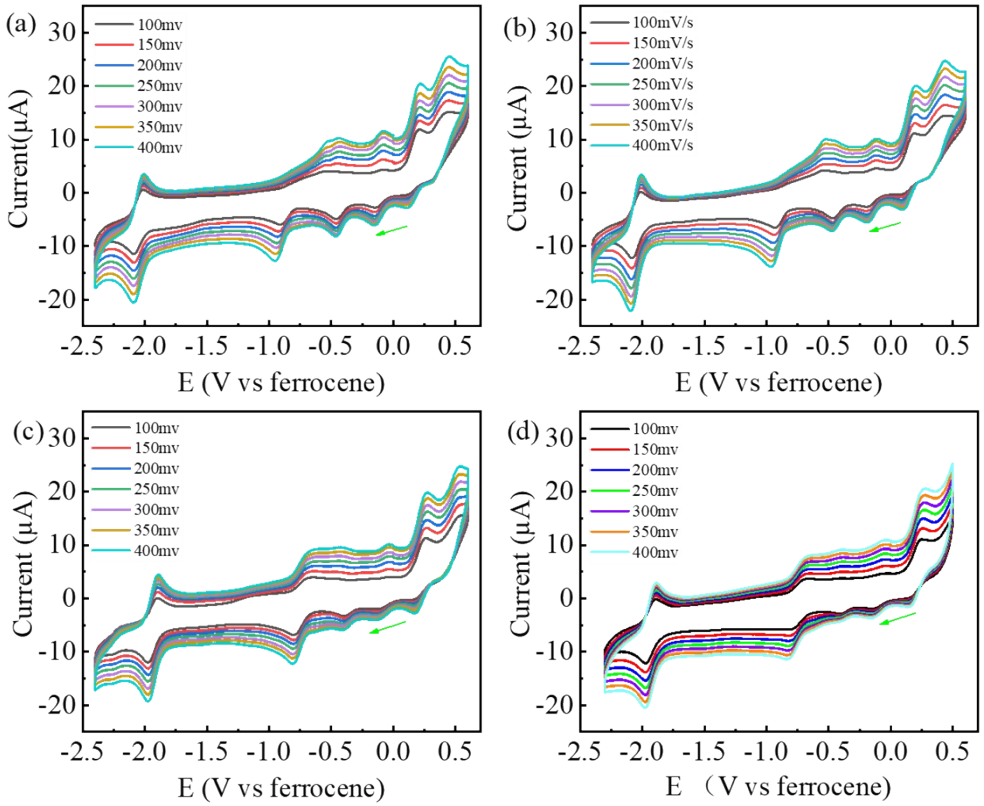

Figure S30 Cobalt complexes **1**, **2**, **3**, **4** (a,b,c,d, 0.6 mM) were test by CV in a varying scan rate (v) from 100 mV/s to 400 mV/s using the glassy carbon as the working electrode

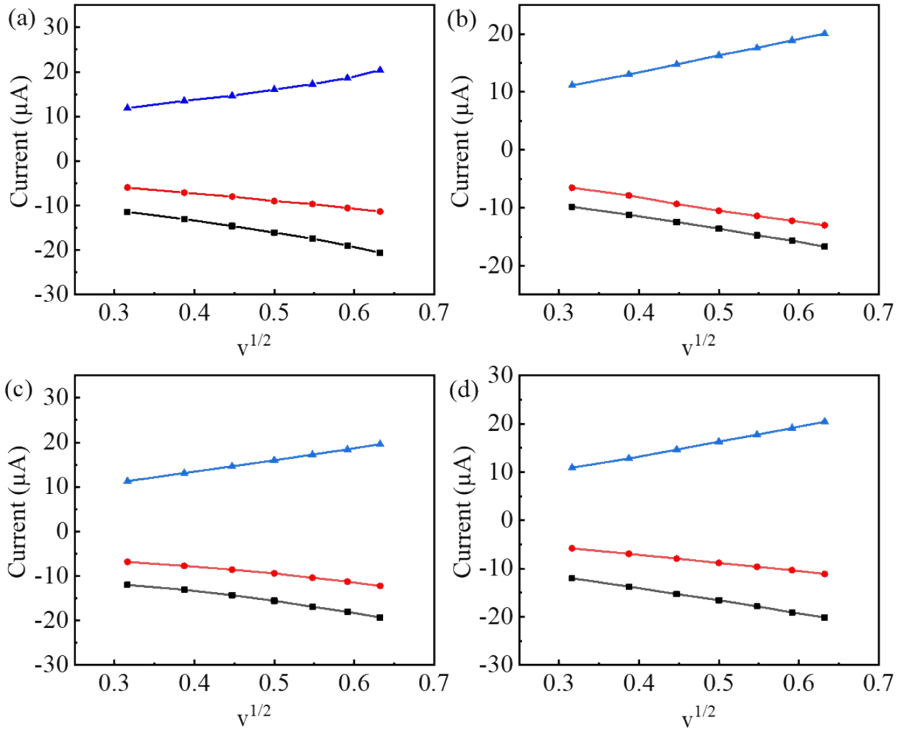

Figure S31 the maximum current (ip) plots of reduction and first oxidation waves *vs.* the scan rate ($v_{1/2}$). Cobalt complex **1**, **2**, **3**, **4** (a, b, c, d)

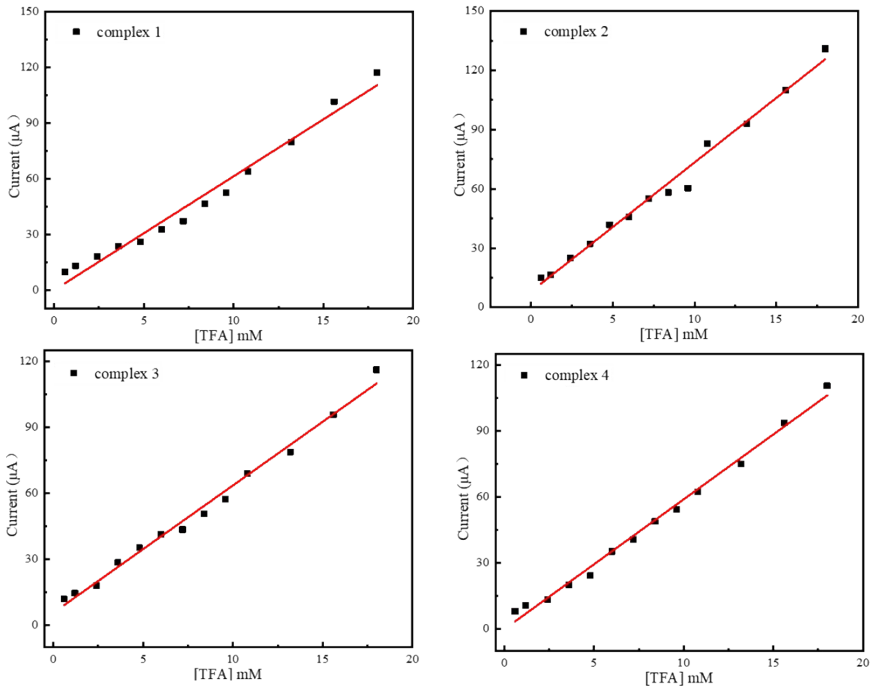

Figure S32 The plot of i_{cat} versus [TFA] for complex **1**,**2**,**3**,**4**

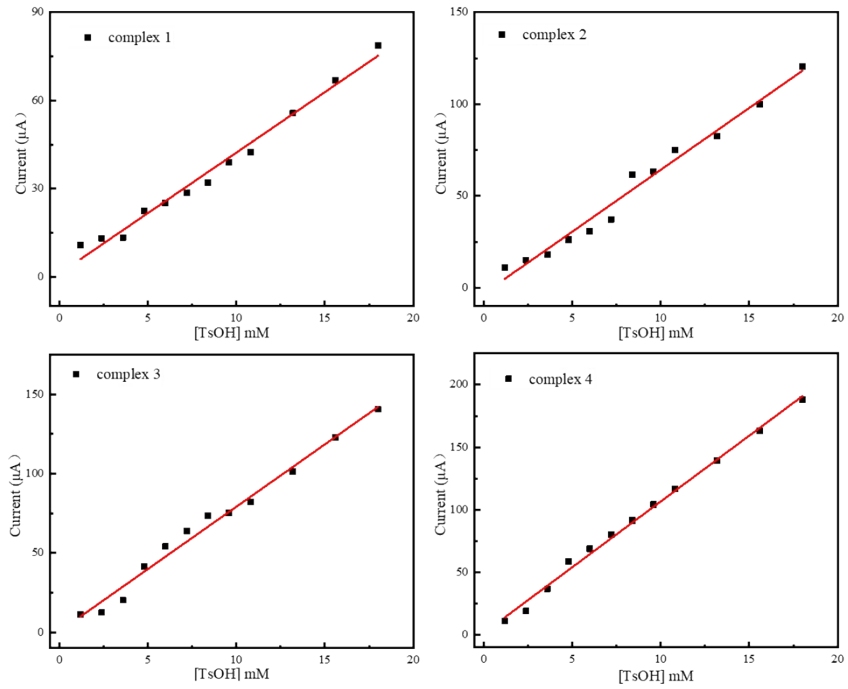

Figure S33 The plot of icat versus [TsOH] for complex **1**,**2**,**3**,**4**

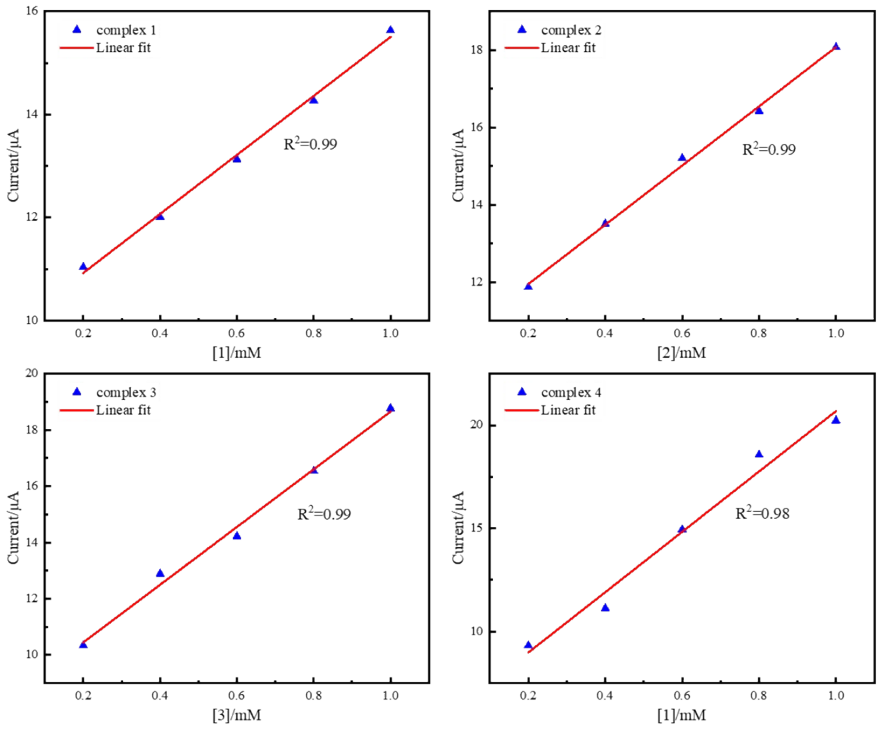

Figure S34 Plot of catalytic current i_{cat} vs. the concentration of **1**, **2**, **3**, **4**. with fixed concentrations of TFA

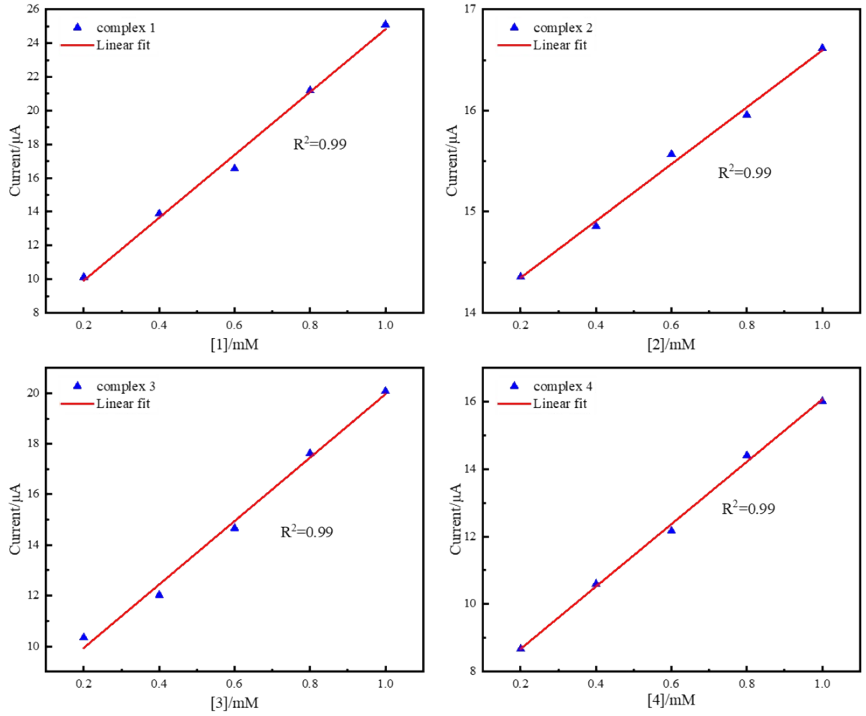

Figure S35 Plot of catalytic current i_{cat} vs. the concentration of **1**, **2**, **3**, **4**. with fixed concentrations of TsOH

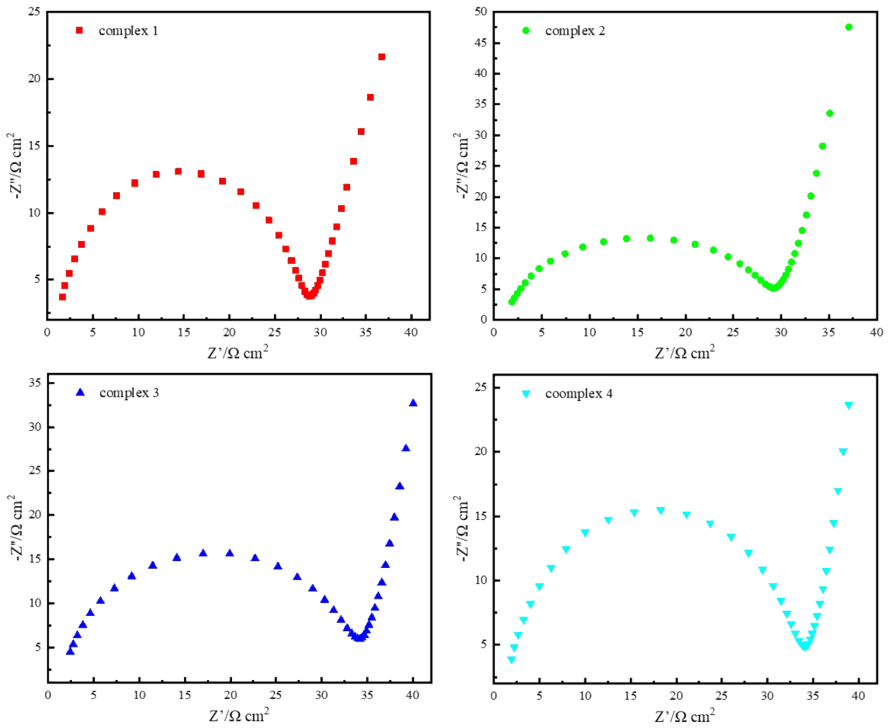

Figure S36 The Nyquist plot for 0.6 mM complex **1**, **2**, **3**, **4** in 0.1M TBAP/DMF with 22 equiv AcOH as external proton source.

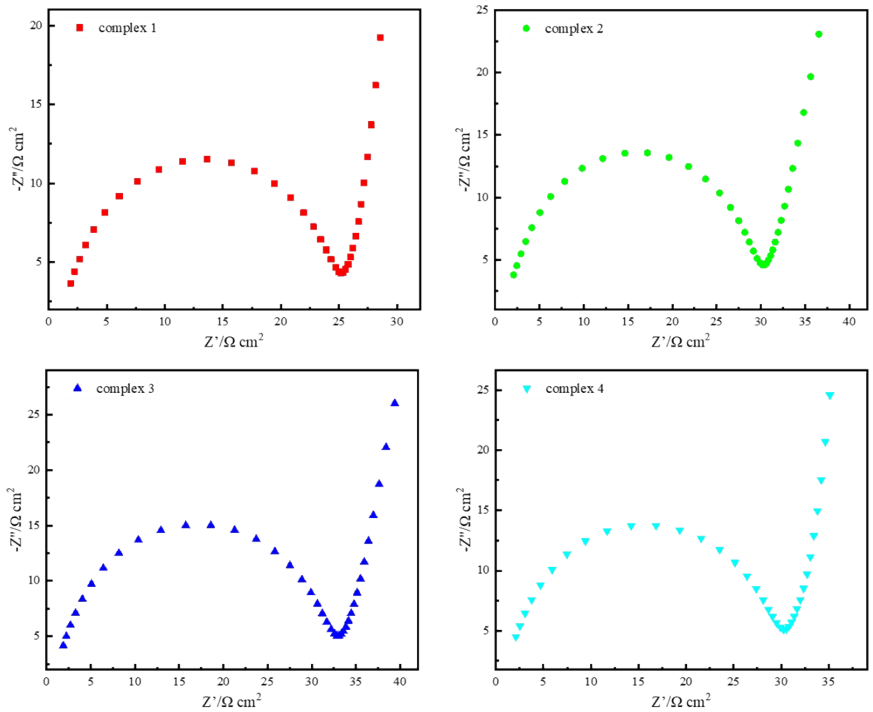

Figure S37 The Nyquist plot for 0.6 mM complex **1**, **2**, **3**, **4** in 0.1M TBAP/DMF with 30 equiv TFA as external proton

source.

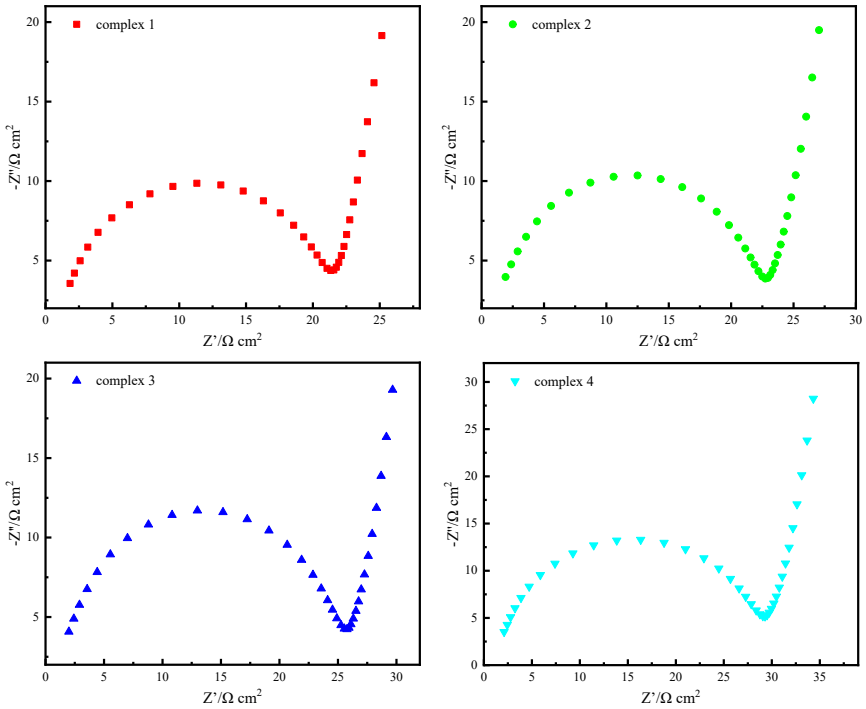

Figure S38 The Nyquist plot for 0.6 mM complex **1**, **2**, **3**, **4** in 0.1 M TBAP/DMF with 30 equiv TsOH as external proton source.

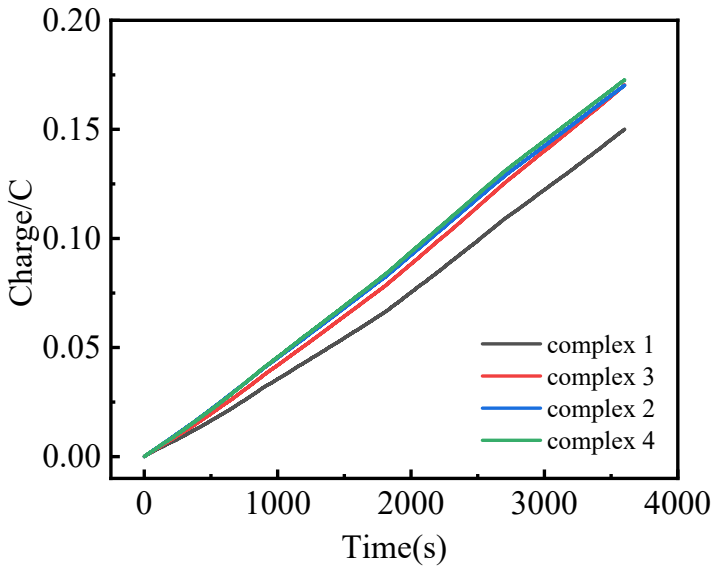

Figure. S39 Charge of complex **1**, **2**, **3**, **4** with the addition of 400 equiv TsOH in DMF over an 1 h electrolysis.

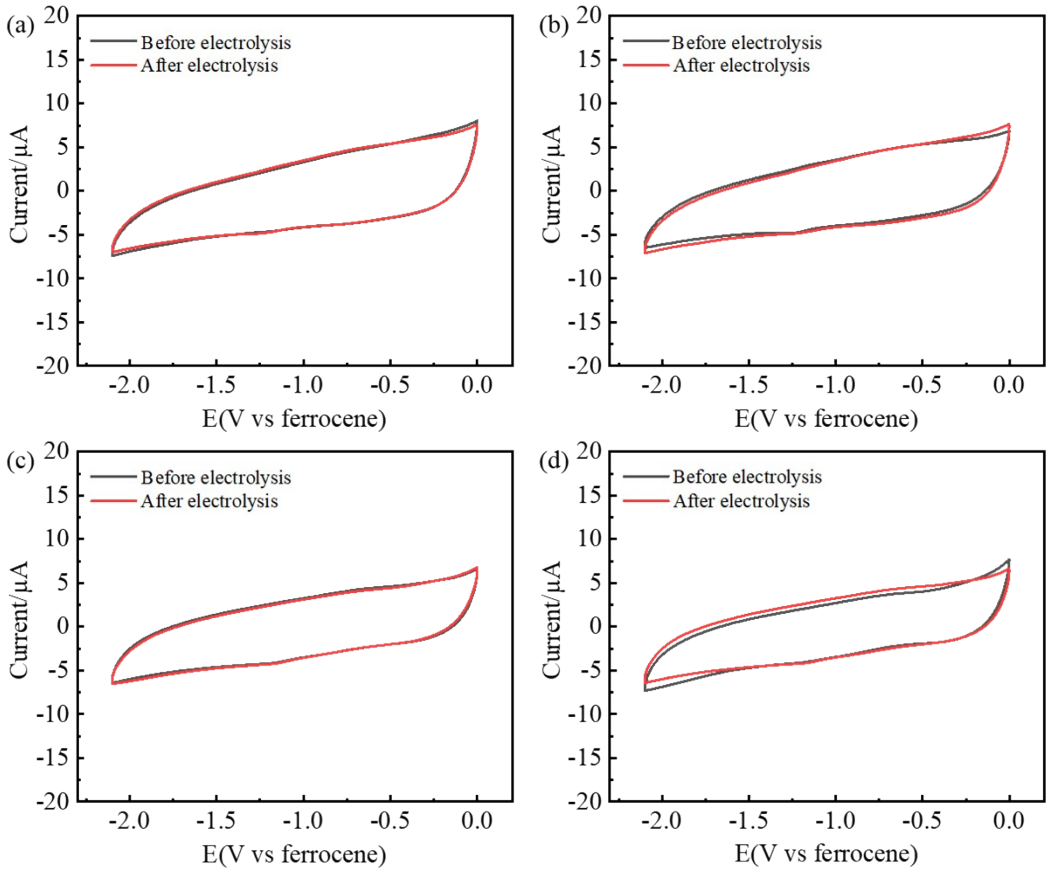

Figure S40 CVs of complex **1**(a),**2**(b),**3**(c),**4**(d) in 0.1M TBAP/DMF at a bare glassy carbon electrode (black line) and the rinsed glassy-carbon electrode after electrochemical measurement (red line).

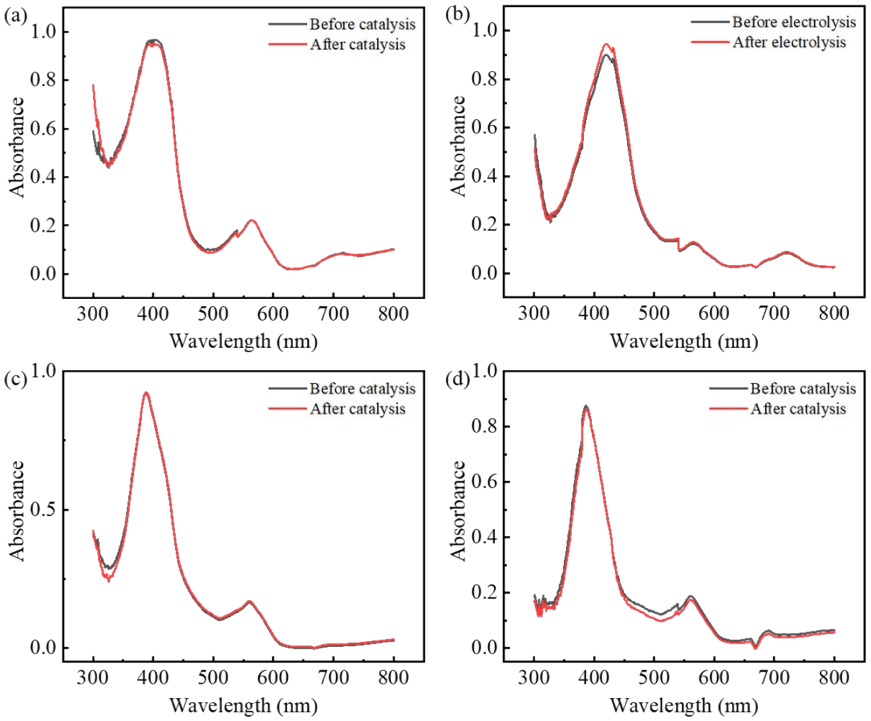

Figure S41 Absorption spectra of complex **1**(a), **2**(b), **3**(c), **4**(d) before (black) and after (red) 2 h electrolysis by applying a voltage of −1.1 V, examined in similar situation (0.1M TBAP/DMF, 400eq TsOH).

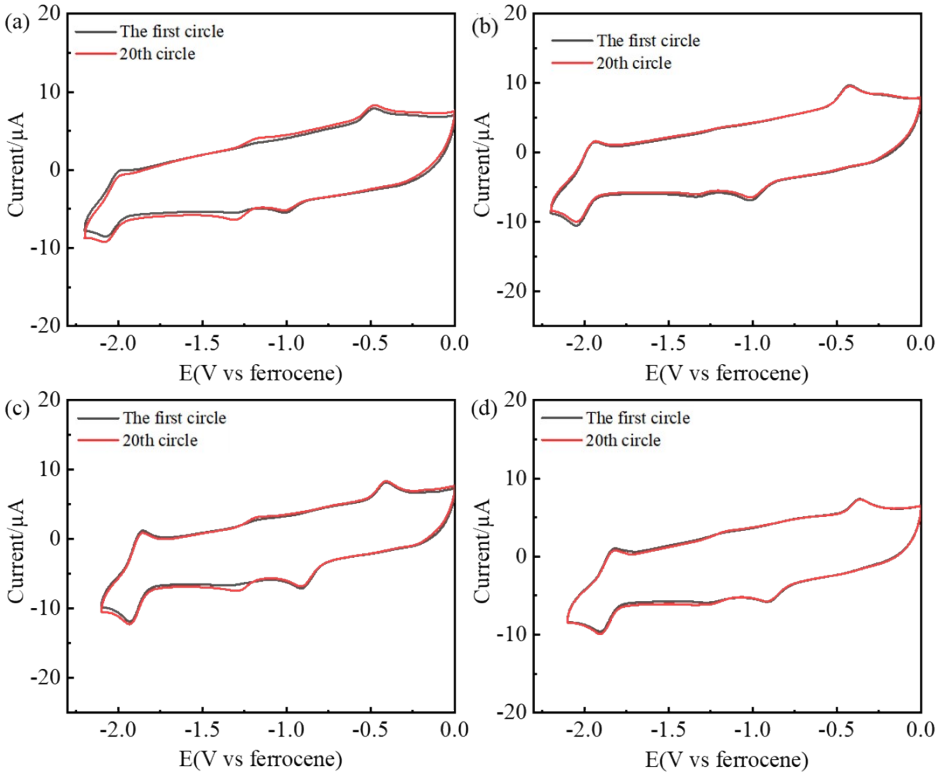

Figure S42 CVs of complex **1**(a),**2**(b),**3**(c),**4**(d) the first circle (black line) and the 20th circle (red line).

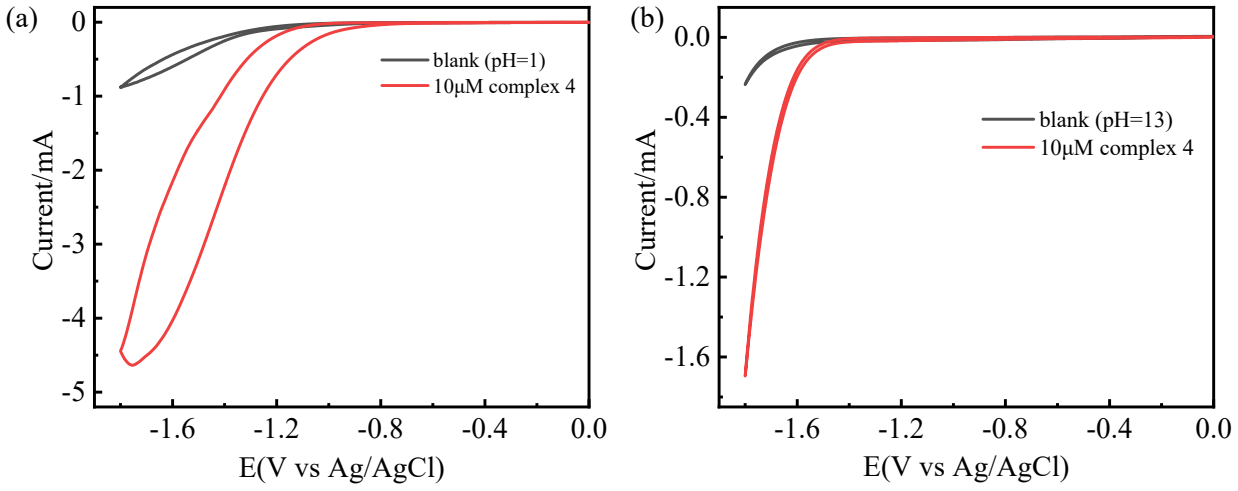

Figure S43. CVs of 10 μM complexes **4** in in nature aqueous medium (a) acidic buffer (pH=1), (b) alkaline buffer (pH=13).

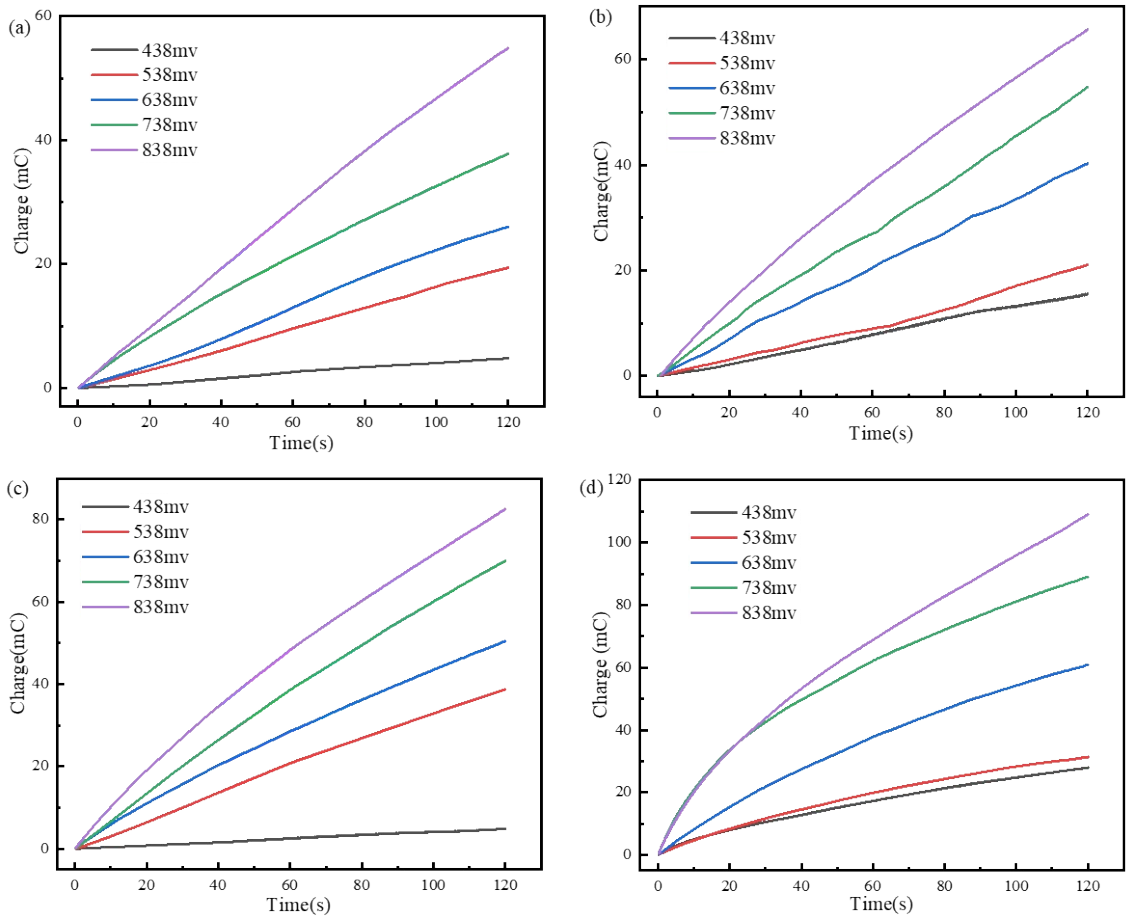

Figure S44 CPE in the different overpotential of 2.5 μM complex **1**, **2**, **3**, **4** (a, b, c, d) in nature aqueous medium all these data were eliminate the blank.

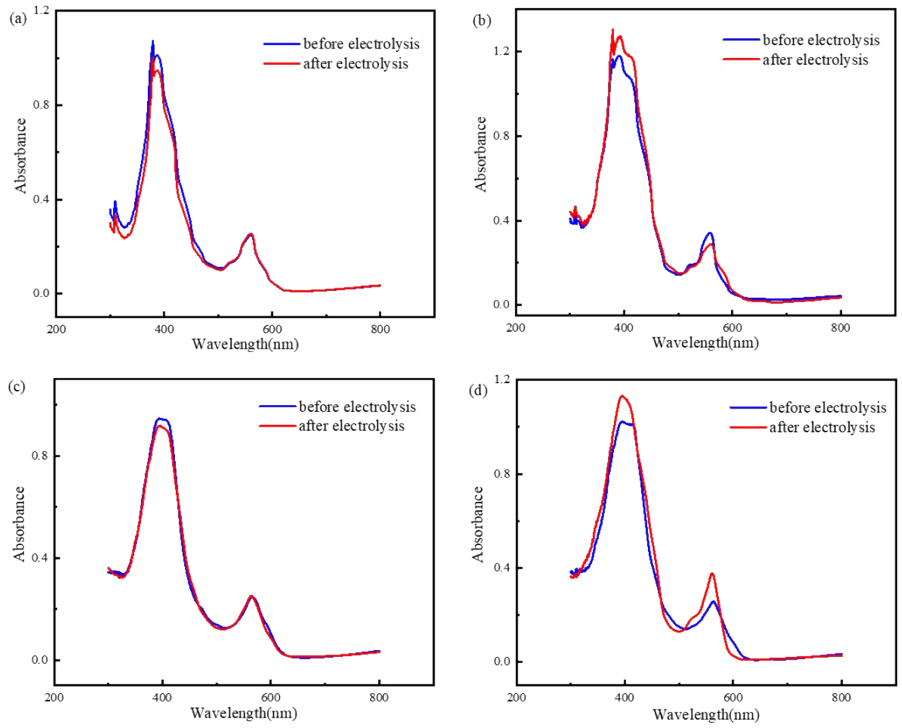

Figure S45 UV-Vis spectra of cobalt complexes **1**, **2**, **3**, **4** (a, b, c, d) before and after 8 h electrolysis with concentration of 2.5μM in nature aqueous medium.

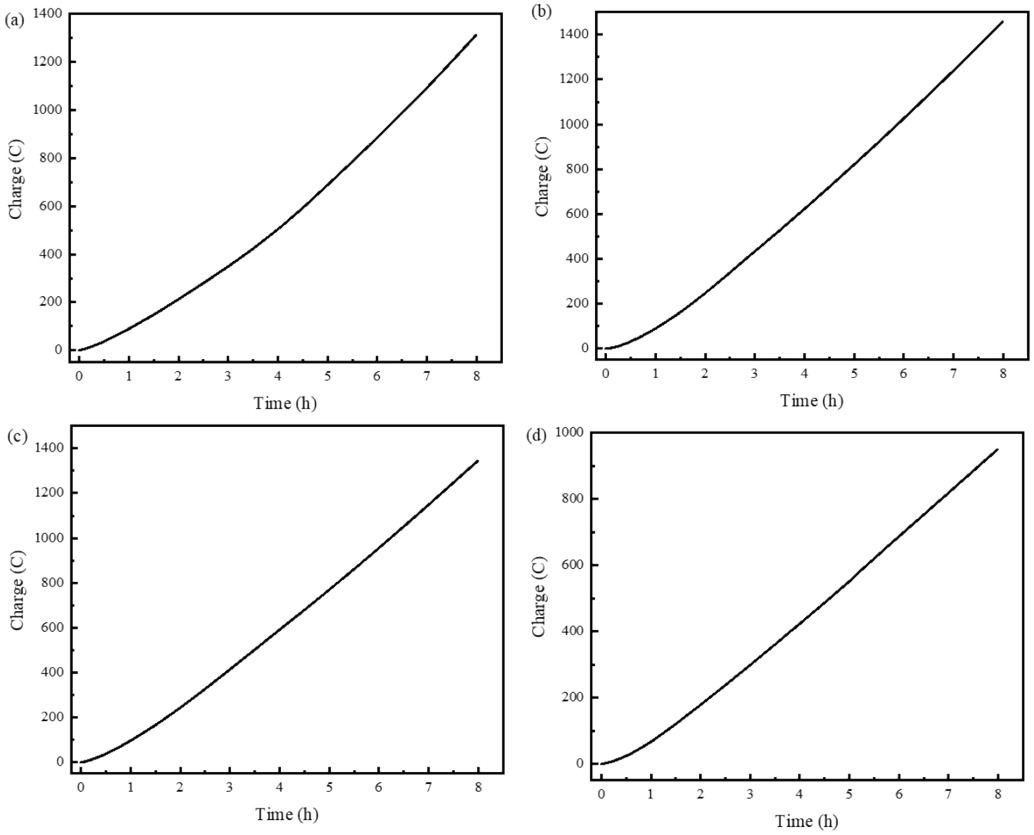

Figure S46 Chronocoulometric of complexes **1**, **2**, **3**, **4** (a, b, c, d, 2.5μM) in nature aqueous medium after 8h electrolysis.

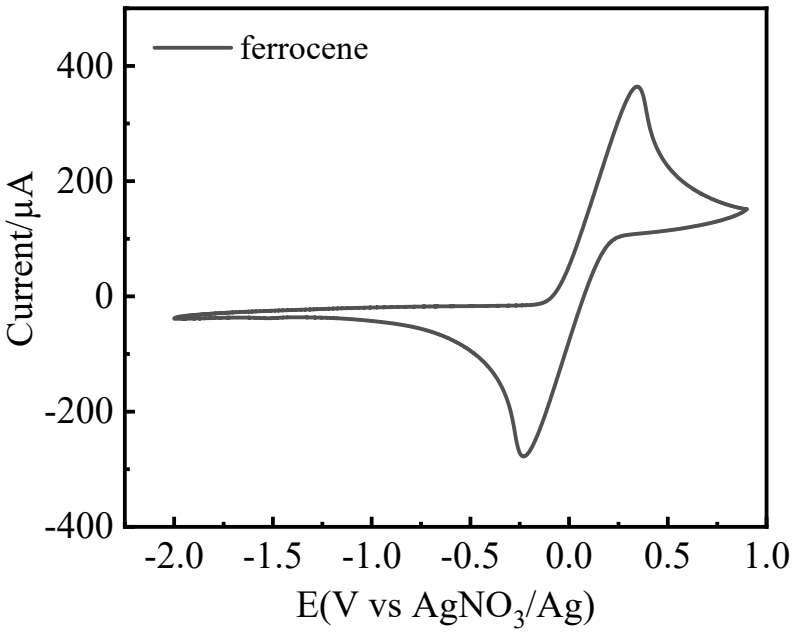

Figure S47 The redox couple of ferrocene with bare GC electrode as working electrode in 0.1M TBAP/DMF

Table S1 Crystal data and structure refinement for complex **3**

Identification code	lzy_0m_sq
Empirical formula	$C_{57}H_{36}CoN_6P$
Formula weight	894.82
Temperature/K	150
Crystal system	triclinic
Space group	P-1
a/Å	14.3899(7)
b/Å	16.2551(8)
c/Å	19.6213(9)
α/°	91.265(2)
β/°	108.634(2)
γ/°	94.679(2)
Volume/Å^3	4328.9(4)
Z	4
ρ_{calc}g/cm^3	1.373
μ/mm^{-1}	0.482
F(000)	1848.0
Crystal size/mm^3	0.12 × 0.08 × 0.05
Radiation	MoKα (λ = 0.71073)
2Θ range for data collection/°	3.88 to 50.054
Index ranges	$-17 \leq h \leq 17$, $-19 \leq k \leq 19$, $-23 \leq l \leq 23$
Reflections collected	45199
Independent reflections	15233 [R_{int} = 0.0941, R_{sigma} = 0.1133]
Data/restraints/parameters	15233/1687/1237
Goodness-of-fit on F^2	1.018
Final R indexes [I>=2σ (I)]	R_1 = 0.0812, wR_2 = 0.1866
Final R indexes [all data]	R1 = 0.1385, wR2 = 0.2263
Largest diff. peak/hole /e Å-3	3.21/-0.85

Table S2 Crystal data and structure refinement for complex **2**

Identification code	RBP_0m
Empirical formula	$C_{56}H_{37}CoN_5P$
Formula weight	869.80
Temperature/K	150
Crystal system	triclinic
Space group	P-1
a/Å	9.7214(18)
b/Å	12.920(2)
c/Å	17.269(3)
α/°	77.514(5)
β/°	83.542(6)
γ/°	79.876(6)
Volume/Å^3	2078.4(7)
Z	2
ρ_{calc}g/cm^3	1.390
μ/mm^{-1}	0.499
F(000)	900.0
Crystal size/mm^3	0.08 × 0.05 × 0.03
Radiation	MoKα (λ = 0.71073)
2Θ range for data collection/°	4.268 to 52.796
Index ranges	$-12 \leq h \leq 11$, $-16 \leq k \leq 16$, $-21 \leq l \leq 21$
Reflections collected	21831
Independent reflections	8338 [R_{int} = 0.1267, R_{sigma} = 0.1867]
Data/restraints/parameters	8338/0/568
Goodness-of-fit on F^2	1.030
Final R indexes [I>=2σ (I)]	R_1 = 0.0810, wR_2 = 0.1323
Final R indexes [all data]	R_1 = 0.1912, wR_2 = 0.1739
Largest diff. peak/hole / e Å^{-3}	0.39/-0.62

Table S3 Selected bond lengths and angles for complex **2**

Bond length, Å		Bond Angle,°	
Co1-P1	2.1967(16)	N1-Co1-N2	89.21(18)
Co1-N1	1.867(4)	N1-Co1-N4	81.19(18)
Co1-N2	1.883(4)	N2-Co1-N3	95.60(18)
Co1-N3	1.882(4)	N3-Co1-N4	88.87(18)
Co1-N4	1.856(4)	P1-Co1-N1	100.93(14)
N5-C1	1.129(7)	P1-Co1-N2	89.21(18)
P1-C40	1.830(6)	P1-Co1-N3	94.84(14)
P1-C46	1.807(5)	P1-Co1-N4	98.98(14)
P1-C51	1.825(5)	N5-C1-C2	177.8(7)

Table S4 Selected bond lengths and angles for complex **3**

Bond length, Å		Bond Angle,°	
Co1-P1	2.1912(17)	N1-Co1-N2	94.8(2)
Co1-N1	1.887(5)	N1-Co1-N4	100.89(14)
Co1-N2	1.885(5)	N2-Co1-N3	89.9(2)
Co1-N3	1.868(5)	N3-Co1-N4	80.8(2)
Co1-N4	1.863(5)	P1-Co1-N1	97.92(15)
N5-C026	1.150(8)	P1-Co1-N2	94.95(15)
N6-C02Q	1.134(9)	P1-Co1-N3	94.95(15)
P1-C00H	1.828(6)	P1-Co1-N4	100.89(14)
P1-C01P	1.832(7)	N5-C026-C01C	179.7(8)
P1-C00O	1.787(6)	N6-C02Q-C01X	178.6(10)

Table S5 Redox potentials of cobalt corroles in DMF (V *vs.* ferrrocene) performed by 0.1 M TBAP

Complex	Couple of Co^{III}/Co^{II}		Couple of Co^{II}/Co^{I}		
	Ox 1, V	Red 1, V	Ox 2, V	Red 2, V	$E_{1/2}$, V
1	-0.511	-0.964	-1.990	-2.068	-2.029
2	-0.474	-0.957	-1.948	-2.026	-1.987
3	-0.428	-0.884	-1.851	-1.924	-1.887
4	-0.392	-0.872	-1.825	-1.897	-1.861

Table S6 H_2 evolving activity by 0.6mM cobalt complex and 18mM (30 equiv) TFA in DMF

Complex	i_{cat}/i_p	E_{cat}, V	Overpotential, mV[a]	TOF, s^{-1}	Efficiency
1	21.15	-2.359	280	86.78	0.70
2	20.48	-2.344	325	98.09	0.75
3	26.50	-2.130	425	136.25	0.88
4	38.95	-2.204	534	294.46	1.29

.

Table S7 H_2 evolving activity by 0.6mM cobalt complex and 18mM (30 equiv) TsOH in DMF

Complex	i_{cat}/i_p	E_{cat}	Overpotential, mV[a]	TOF, s^{-1}	Efficiency
1	14.81	-2.359	241	42.56	0.49
2	20.25	-2.344	272	79.58	0.67
3	30.84	-2.342	326	184.51	1.02
4	44.33	-2.359	486	381.37	1.47

a As determined by the method of Evans for calculating overpotentials.[1]

Table S8 HER TOF for transition metal corrole in organic solvent by using organic acids as proton

Complex	TOF	Proton resource	Solution	Reference
1	42 s^{-1}	TsOH	DMF	This work
2	79 s^{-1}	TsOH	DMF	This work
3	184 s^{-1}	TsOH	DMF	This work
4	381 s^{-1}	TsOH	DMF	This work
$((CF_3)_3$-tpfc)Cu	356 s^{-1}	TFA	Acetonitrile	[2]
$((CF_3)_4$-tpfc)Cu	227 s^{-1}	TFA	Acetonitrile	[2]
(tpfc)MoV(O)	23 s^{-1}	DMF-H^+	DMF	[3]
(tpfc)MoV(O)Br_8	2.48 s^{-1}	DMF-H^+	DMF	[3]
(4-BPFC)Co	93.15 s^{-1}	TsOH	DMF	[4]
(3-BPSC)Co	187.61 s^{-1}	TsOH	DMF	[4]

Table S9 TOF of transition metal complexes in nature homogeneous aqueous solution

Complex	TOF	Overpotential(mV)	Solution	Reference
1	388.3 h^{-1}	838	Buffer	This work
2	698.9 h^{-1}	838	Buffer	This work
3	723.5 h^{-1}	838	Buffer	This work
4	1657.9 h^{-1}	838	Buffer	This work
Fe(TPFC)Cl	274.2 h^{-1}	838	Water	[5]
Cu(HL)Cl	482.0 h^{-1}	837.6	Buffer	[6]
$[Ni\text{-}en\text{-}P_2](ClO_4)_2$	1327 h^{-1}	837.6	Buffer	[7]
$[Ni(HL\text{-}Cl)_2]$	574 h^{-1}	837.6	Buffer	[8]

1. G. A. Felton, R. S. Glass, D. L. Lichtenberger and D. H. Evans, *Inorg Chem*, 2006, **45**, 9181-9184.
2. K. Sudhakar, A. Mahammed, Q.-C. Chen, N. Fridman, B. Tumanskii and Z. Gross, *ACS Applied Energy Materials*, 2020, **3**, 2828-2836.
3. P. Yadav, I. Nigel-Etinger, A. Kumar, A. Mizrahi, A. Mahammed, N. Fridman, S. Lipstman, I. Goldberg and Z. Gross, *iScience*, 2021, **24**, 102924.
4. J.-J. Fang, J. Lan, G. Yang, G.-Q. Yuan, H.-Y. Liu and L.-P. Si, *New Journal of Chemistry*, 2021, **45**, 5127-5136.
5. Y.-Q. Zhong, M. S. Hossain, Y. Chen, Q.-H. Fan, S.-Z. Zhan and H.-Y. Liu, *Transition Metal Chemistry*, 2019, **44**, 399-406.
6. R. Z. Liao, M. Wang, L. Sun and P. E. Siegbahn, *Dalton Trans*, 2015, **44**, 9736-9739.
7. C.-L. Wang, H. Yang, J. Du and S.-Z. Zhan, *International Journal of Hydrogen Energy*, 2021, **46**, 32480-32489.
8. J. Du, H. Yang, C.-L. Wang and S.-Z. Zhan, *Molecular Catalysis*, 2021, **516**.